



NAVAL POSTGRADUATE SCHOOL

MONTEREY, CALIFORNIA

THESIS

**A DOUBLE-POLE HIGH VOLTAGE HIGH CURRENT
SWITCH**

by

Dagmara W. Moselle

December 2005

Thesis Advisor:
Co-Advisor:

William B. Maier II
Peter P. Crooker

Approved for public release; distribution is unlimited

THIS PAGE INTENTIONALLY LEFT BLANK

REPORT DOCUMENTATION PAGE			<i>Form Approved OMB No. 0704-0188</i>	
Public reporting burden for this collection of information is estimated to average 1 hour per response, including the time for reviewing instruction, searching existing data sources, gathering and maintaining the data needed, and completing and reviewing the collection of information. Send comments regarding this burden estimate or any other aspect of this collection of information, including suggestions for reducing this burden, to Washington headquarters Services, Directorate for Information Operations and Reports, 1215 Jefferson Davis Highway, Suite 1204, Arlington, VA 22202-4302, and to the Office of Management and Budget, Paperwork Reduction Project (0704-0188) Washington DC 20503.				
1. AGENCY USE ONLY (Leave blank)		2. REPORT DATE December 2005	3. REPORT TYPE AND DATES COVERED Master's Thesis	
4. TITLE AND SUBTITLE: A Double-Pole High Voltage High Current Switch			5. FUNDING NUMBERS	
6. AUTHOR(S) Dagmara W. Moselle				
7. PERFORMING ORGANIZATION NAME(S) AND ADDRESS(ES) Naval Postgraduate School Monterey, CA 93943-5000			8. PERFORMING ORGANIZATION REPORT NUMBER	
9. SPONSORING /MONITORING AGENCY NAME(S) AND ADDRESS(ES) N/A			10. SPONSORING/MONITORING AGENCY REPORT NUMBER	
11. SUPPLEMENTARY NOTES The views expressed in this thesis are those of the author and do not reflect the official policy or position of the Department of Defense or the U.S. Government.				
12a. DISTRIBUTION / AVAILABILITY STATEMENT Approved for public release; distribution is unlimited			12b. DISTRIBUTION CODE	
13. ABSTRACT (maximum 200 words) Substantial research has been done to find the best power supply to drive the Naval railgun. Inertial energy storage using rotating machines, high voltage and low voltage capacitors, and batteries have been candidates. Low voltage capacitors and batteries are, or may soon be, possible energy sources. These low voltage energy sources would require a pulse forming inductive network (PFIN) to transform the low-voltage electrical energy to power appropriate for the railgun. The PFIN electrical setup requires an opening switch that would carry high currents (50 kA) for times greater than 0.1 seconds and that could open against such high currents (circuit interruption). This thesis proposes a mechanical vacuum switch with an externally applied magnetic field to divert charged particles to an auxiliary electrode. A prototype switch suitable for ≈ 5 kA has been designed but not yet tested. Computational results suggest that very large magnetic fields ($>1T$) may be required to divert heavy charged particles, e.g. Cu^+ .				
14. SUBJECT TERMS Double-Pole, Pulse Forming Inductive Network, PFIN, Railgun, Inductive Storage			15. NUMBER OF PAGES 68	
			16. PRICE CODE	
17. SECURITY CLASSIFICATION OF REPORT Unclassified	18. SECURITY CLASSIFICATION OF THIS PAGE Unclassified	19. SECURITY CLASSIFICATION OF ABSTRACT Unclassified	20. LIMITATION OF ABSTRACT UL	

THIS PAGE INTENTIONALLY LEFT BLANK

Approved for public release; distribution is unlimited

A DOUBLE-POLE HIGH VOLTAGE HIGH CURRENT SWITCH

Dagmara W. Moselle
Lieutenant, United States Navy
B.S., Pennsylvania State University, 1999

Submitted in partial fulfillment of the
requirements for the degree of

MASTER OF SCIENCE IN APPLIED PHYSICS

from the

**NAVAL POSTGRADUATE SCHOOL
December 2005**

Author: Dagmara Moselle

Approved by: William B. Maier II
Thesis Advisor

Peter P. Crooker
Co-Advisor

James Luscombe
Chairman, Department of Physics

THIS PAGE INTENTIONALLY LEFT BLANK

ABSTRACT

Substantial research has been done to find the best power supply to drive the Naval railgun. Inertial energy storage using rotating machines, high voltage and low voltage capacitors, and batteries have been candidates. Low voltage capacitors and batteries are, or may soon be, possible energy sources. These low voltage energy sources would require a pulse forming inductive network (PFIN) to transform the low-voltage electrical energy to power appropriate for the railgun. The PFIN electrical setup requires an opening switch that would carry high currents (50 kA) for times greater than 0.1 seconds and that could open against such high currents (circuit interruption). This thesis proposes a mechanical vacuum switch with an externally applied magnetic field to divert charged particles to an auxiliary electrode. A prototype switch suitable for ≈ 5 kA has been designed but not yet tested. Computational results suggest that very large magnetic fields (>1 T) may be required to divert heavy charged particles, e.g. Cu^+ .

THIS PAGE INTENTIONALLY LEFT BLANK

TABLE OF CONTENTS

I.	INTRODUCTION AND BACKGROUND.....	1
A.	RAILGUN POWER SYSTEM PROBLEM.....	1
B.	BASIC PFIN OPERATION.....	1
C.	TYPES OF POWER SUPPLIES	2
D.	SWITCHES	3
1.	Types of Switches for Railgun Application	3
a.	<i>Solid State</i>	<i>3</i>
b.	<i>Hybrid</i>	<i>4</i>
c.	<i>Vacuum Interrupter</i>	<i>4</i>
II.	DESIGN CONCEPT.....	7
A.	CLOSED SWITCH.....	7
B.	OPENED SWITCH	8
III.	PROTOTYPE SWITCH	11
A.	SWITCH DESIGN.....	11
1.	Sputter-Ion Vacuum Pump Housing.....	12
2.	FEMLAB Simulations	13
a.	<i>Electron Trajectory</i>	<i>13</i>
b.	<i>Copper Ion Trajectory.....</i>	<i>15</i>
B.	SWITCH ACTIVATION	21
1.	Hand Calculation of Necessary Force to Retract the Electrode	22
C.	SWITCH TEST CONCEPT	23
1.	Component Design Considerations	23
a.	<i>Inductor Design Specifics.....</i>	<i>23</i>
2.	P-Spice Simulation and Analysis	24
a.	<i>SW1 Switch Analysis for Closed Circuit</i>	<i>24</i>
b.	<i>SW1 Switch Analysis for Opened Circuit</i>	<i>25</i>
3.	Theoretical Model and Considerations	25
IV.	CONCLUSION	29
V.	FUTURE WORK	31
	APPENDIX A. ASSEMBLY DRAWINGS (O-RING GROOVES, THREADS AND SOME BOLT HOLES ARE OMITTED).....	33
	APPENDIX B. PROTOTYPE APPLICATION	41
A.	DESCRIPTION OF THE PROBLEM(S) THE INVENTION ADDRESSES	42
B.	DESCRIPTION OF THE PRIOR ART TECHNOLOGY THAT DID NOT FULLY RESOLVE THE PROBLEM(S) ADDRESSED BY THE PRESENT INVENTION BUT THAT MAY HAVE COME CLOSE	42

C.	SCHEMATIC AND BRIEF STEP-BY-STEP DESCRIPTION AND EXPLANATION OF THE INVENTION.....	43
D.	EXISTING PHOTOGRAPHS, DRAWINGS, SCHEMATICS, AND OTHER MATERIAL THAT PROVIDES INSIGHT TO THE INVENTION, HOW IT FUNCTIONS, AND WHAT IT DOES	47
E.	IN ANTICIPATION OF POSSIBLE COMMERCIAL LICENSING UNDER THE TECHNOLOGY TRANSFER ACT, PLEASE IDENTIFY ANY SPONSORS (GOV'T OR COMMERCIAL COMPANIES) KNOWN TO HAVE AN INTEREST IN THE INVENTION. PROVIDE ADDRESS AND GEOGRAPHICAL LOCATION IF KNOWN.....	47
F.	WAS THIS INVENTION DONE UNDER A COOPERATIVE RESEARCH AND DEVELOPMENT AGREEMENT?	47
G.	OTHER POTENTIAL USES BESIDES RAILGUN POWER SYSTEMS.....	47
H.	NOTE ON OTHER EXISTING TECHNOLOGY	47
	APPENDIX C. LONG THIN SOLENOID.....	49
	LIST OF REFERENCES.....	51
	INITIAL DISTRIBUTION LIST	53

LIST OF FIGURES

Figure 1.	Simple battery PFIN schematic.	2
Figure 2.	Basic vacuum interrupter. [3]	5
Figure 3.	Arc example. [3]	6
Figure 4.	Closed switch. Magnetic field not shown. The tertiary electrode can be connected to ground through a biased capacitor or other circuit.	7
Figure 5.	Opened switch.....	8
Figure 6.	Opened switch without applied magnetic field.....	9
Figure 7.	Prototype switch.....	11
Figure 8.	Vacuum ion pump before modification. (The locations of the planned modifications are indicated.).....	12
Figure 9.	Side view of electron trajectory within the cylindrically symmetric switch. Transparent view. (Some extraneous lines used by FEMLAB are shown but have no affect on the results.) Important components are labeled.....	14
Figure 10.	Electron trajectory looking from the retractable rod perspective; slightly off axis. (Some extraneous lines used by FEMLAB are shown but have no affect on the results.) Important components are labeled.	15
Figure 11.	Side view of copper ion trajectory starting near bottom of anode within the cylindrically symmetric switch. (Some extraneous lines used by FEMLAB are shown but have no affect on the results.) Important components are labeled.....	16
Figure 12.	Side view of copper ion trajectory starting near middle of anode within the cylindrically symmetric switch. (Some extraneous lines used by FEMLAB are shown but have no affect on the results.) Important components are labeled.....	16
Figure 13.	Side view of copper ion trajectory starting near top of anode within the cylindrically symmetric switch. (Some extraneous lines used by FEMLAB are shown but have no affect on the results.) Important components are labeled.....	17
Figure 14.	Electric field strength along red line near anode.	18
Figure 15.	Electric field strength along red line midway between main electrodes.	19
Figure 16.	Electric field strength along red line near cathode.....	20
Figure 17.	Spring activation assembly.	21
Figure 18.	Suggested triggering mechanism.	22
Figure 19.	P-Spice railgun battery PFIN test circuit.	24
Figure 20.	P-Spice battery PFIN test circuit of current vs time.	25
Figure 21.	Theoretical railgun battery PFIN schematic.	26
Figure 22.	Dimensionless current, $\frac{I}{\left(\frac{V_B}{R}\right)}$, versus dimensionless time, $\frac{R}{L}t$	27

Figure 23.	Ratio of inductor energy to battery energy, $\frac{W_L}{W_B}$, versus dimensionless time, $\frac{R}{L}t$	28
Figure 24.	Prototype switch w/ vacuum ion pump pod and magnetic plates.....	33
Figure 25.	Top view of prototype switch w/ vacuum ion pump pod and w/out magnetic plates.....	33
Figure 26.	Front view of prototype switch w/ vacuum ion pump pod and magnetic plates.	34
Figure 27.	Right view of prototype switch w/ vacuum ion pump pod and magnetic plates. (Some vertical lines are distorted in the side view due to the drawing program.).....	34
Figure 28.	Retractable rod.	35
Figure 29.	Tertiary electrode.....	35
Figure 30.	Top and bottom main electrodes.....	36
Figure 31.	Top flange.	36
Figure 32.	Second flange from top.....	37
Figure 33.	Third flange from top.....	37
Figure 34.	Mounting bottom plate w/ feed through hole and stationary rod hole.....	38
Figure 35.	Bottom lower extension box.	38
Figure 36.	Bottom flange.....	39
Figure 37.	Top and bottom insulators.	39

ACKNOWLEDGMENTS

I send my gratitude to Professor Bill Maier and Mr. Don Snyder for their limitless patience and time in the lab. Also I give my husband, Greg, my deepest thankfulness for his unwavering love and support.

THIS PAGE INTENTIONALLY LEFT BLANK

I. INTRODUCTION AND BACKGROUND

A. RAILGUN POWER SYSTEM PROBLEM

Navy's future to combat modern day adversaries has changed the demands of weaponry design. The Navy's precision strike railgun will be able to provide direct and indirect fire support to the horizon or several hundred nautical miles within minutes. It will undoubtedly be an invaluable asset to any field commander in times of war. To design a high performance railgun system there still remain some major design parameters that need to be improved upon to meet operational criteria, including rail erosion, fire-control and guidance, and the pulsed power supply.

Substantial research has been done to find the best power supply. Candidates have included rotating machines, high voltage and low voltage capacitors, and batteries. In the past, low voltage capacitors and batteries were not considered adequate due to their low energy and power densities. Recently technological advancements have made these components a possible source of energy within a Pulse Forming Inductive Network (PFIN). Utilizing the PFIN electrical setup to provide better power supplies for an operational railgun still requires an opening switch that would carry high currents (>50 kA) for times greater than 0.1 seconds and could open against such high currents (circuit interruption). This thesis will address a double pole mechanical switch to be used in conjunction with low voltage batteries to drive the Navy's railgun.

B. BASIC PFIN OPERATION

A pulse forming inductive network's function is to store electrical energy and then release the energy on demand to the railgun. The notional requirements for the Navy railgun are 64 MJ at the muzzle, which requires the PFIN to provide 20 GW for a few milliseconds. [1] A simplified schematic of a PFIN is shown in Figure 1.

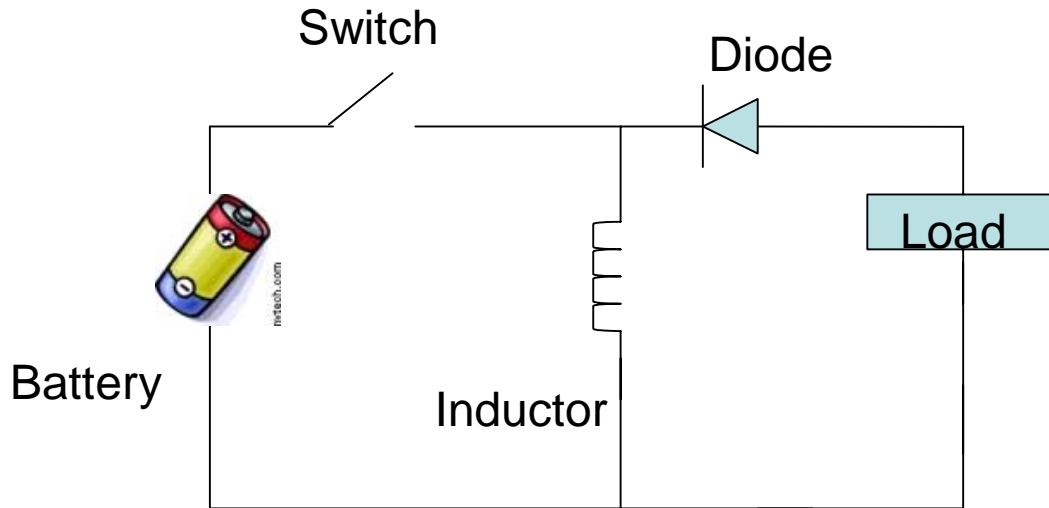


Figure 1. Simple battery PFIN schematic.

Assume the switch is closed instantaneously at time zero. The charging phase of the inductor begins when current flows from the battery bank to the inductor and the battery's chemical energy is stored as magnetic field. While the switch is closed, the PFIN can be modeled as an LR battery circuit. The time required to energize the inductor can be long (~ 1 s).

The discharging phase of the inductor begins when the switch is opened and the battery no longer supplies current. When this occurs, the collapsing magnetic field in the inductor will drive current through the railgun, which has very low impedance. Ultimately, an opening switch needs to be developed to carry large currents (>90 kA) for long periods of time (> 0.1 s).

C. TYPES OF POWER SUPPLIES

There are four major energy storage types being considered for the railgun power storage design: high voltage (HV) capacitors, low voltage capacitors, Inertial Energy Storage flywheel (compulsators) and batteries.

High voltage capacitors can store approximately 1 MJ/m^3 , however, it is a bulky manner to store energy. In addition, the HV capacitor lifetime is too short for shipboard use. HV capacitors with higher energy density are being developed.

The flywheel design has even greater energy density at about 40-50 MJ/m³, but the effective energy efficiency is 20-25%. [2] Flywheels undergo enormous centrifugal stress to store the amount of energy required to operate a railgun, and even larger stress when the railgun load is applied. Significant technological advancements need to be made in structural and material design to provide power to the railgun. In addition, compulsators will need considerable maintenance due to their complexity.

Low voltage capacitors and batteries are viable energy storage supplies that could drive the railgun. Low voltage capacitors can provide up to 100 J/g at low voltages (less than 3V). [2] These capacitors can be online for months at a time and be cycled on and off repeatedly without degrading performance. However, commercially manufactured available low voltage capacitors are not suitable for a PFIN system at this time due to their high equivalent series resistance (ESR). For a 200 MJ PFIN storage system, currently available low voltage capacitors may have less than 5% energy transfer efficiency. [2] Low voltage batteries are not suitable to drive the railgun directly, but adapting them in the Pulse Forming Inductive Network may produce sufficient power to fire the railgun. In either low voltage electrical storage device, the battery or capacitor may require a switch that can carry large currents for long periods of time.

D. SWITCHES

1. Types of Switches for Railgun Application

a. Solid State

Solid state switches are fast acting switches that work with accurate timing and can be concatenated to perform as one switch. They require minimal maintenance over long periods of repetitive operation and avoid the arc-extinguishing problem associated with mechanical switches. To transfer power to the railgun, it would take several thousand solid state switches assembled in a bulky switching construction. [2] In addition, commercially available solid state switches are capable of supplying 90 kA for short periods of time and can interrupt current to approximately 5 kA. However, they can not support adequate operating times (> 0.1 s) appropriate for a railgun powered by batteries and a PFIN. [3]

b. Hybrid

Hybrid switches operate with low conduction and small switching losses when designed with a semiconductor or fuse. [4] Current conducts through a main switch (vacuum interrupter or other robust switch) for an extended time; when the switch is to be opened, a counter pulse diverts current through a capacitor while the main switch opens. Hybrid arrangements in combination with a vacuum switch have been shown to break current up to 40 kA in the laboratory. [4] For the purpose of railgun operating requirements, hybrid switches would require substantial space because they need to be arranged in parallel for proper circuit interruption and they are fairly bulky and complex.

c. Vacuum Interrupter

Vacuum interrupters can operate up to 40 kA for reasonably long periods of time (≥ 0.5 s). [5] Since they are mechanical switches, they are rather compact, sturdy and rugged. Due to their vacuum clean environment, they require minimal maintenance and upkeep. They have good timing characteristics and are usually compact in size. Vacuum interrupters function on the notion that as the current decreases to zero within the vacuum, the metallic vapor from the electrodes condenses rapidly so that there is no medium to sustain the discharge between the electrodes. Currently, vacuum interrupters turn off low currents well, but their design needs to be modified to break high current. Figure 2 shows a schematic of a typical commercial vacuum interrupter and its major components.

- 1 Stem/terminal
- 2 Metal bellows
- 3 Interrupter lid
- 4 Ceramic insulator
- 5 Shield
- 6 Contacts
- 7 Stem
- 8 Interrupter lid

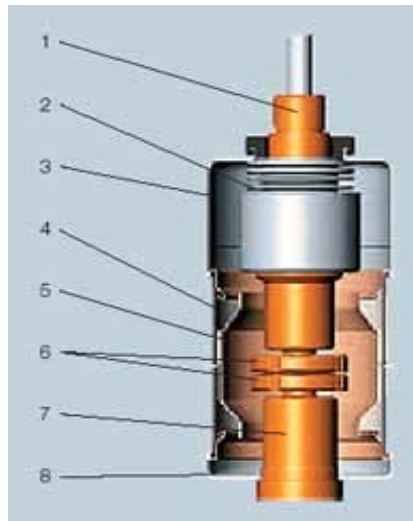


Figure 2. Basic vacuum interrupter. [3]

(1) Formation of a Vacuum Arc. As the switch is opened and the main cathode and anode separate, an arc develops due to the rapid rise in voltage caused by the sudden change in current through the circuit inductance. The arc may appear as seen in Figure 3. When molecular velocities increase enough to heat the discharge, thermal ionization occurs and plasma is formed. These ionized particles include electrons and charged ions from the electrode material. Current flow may continue between the cathode and anode until the particles are fully re-condensed and the current is approximately zero. Typical arcing potentials range from few tens of volts to a few hundred volts between the electrode plates.



Figure 3. Arc example. [3]

(2) Direct Current Interruption in Vacuum Arcs. Direct current interruption is more challenging than in an alternating current system because it does not have a natural zero value of current. Therefore, there exists a need to impose a condition to aid in the suppression of the arc. A magnetic field applied perpendicular to the electric field will disrupt the initial particle trajectories and cause the particles to drift perpendicular to the direction of the electric field between the switched electrodes.

II. DESIGN CONCEPT

A. CLOSED SWITCH

The double-pole switch depicted in Figure 4 is designed to operate under vacuum conditions. When the switch is closed, current will flow through the switch with minimal resistance and provide power to the load as seen in Figure 4.

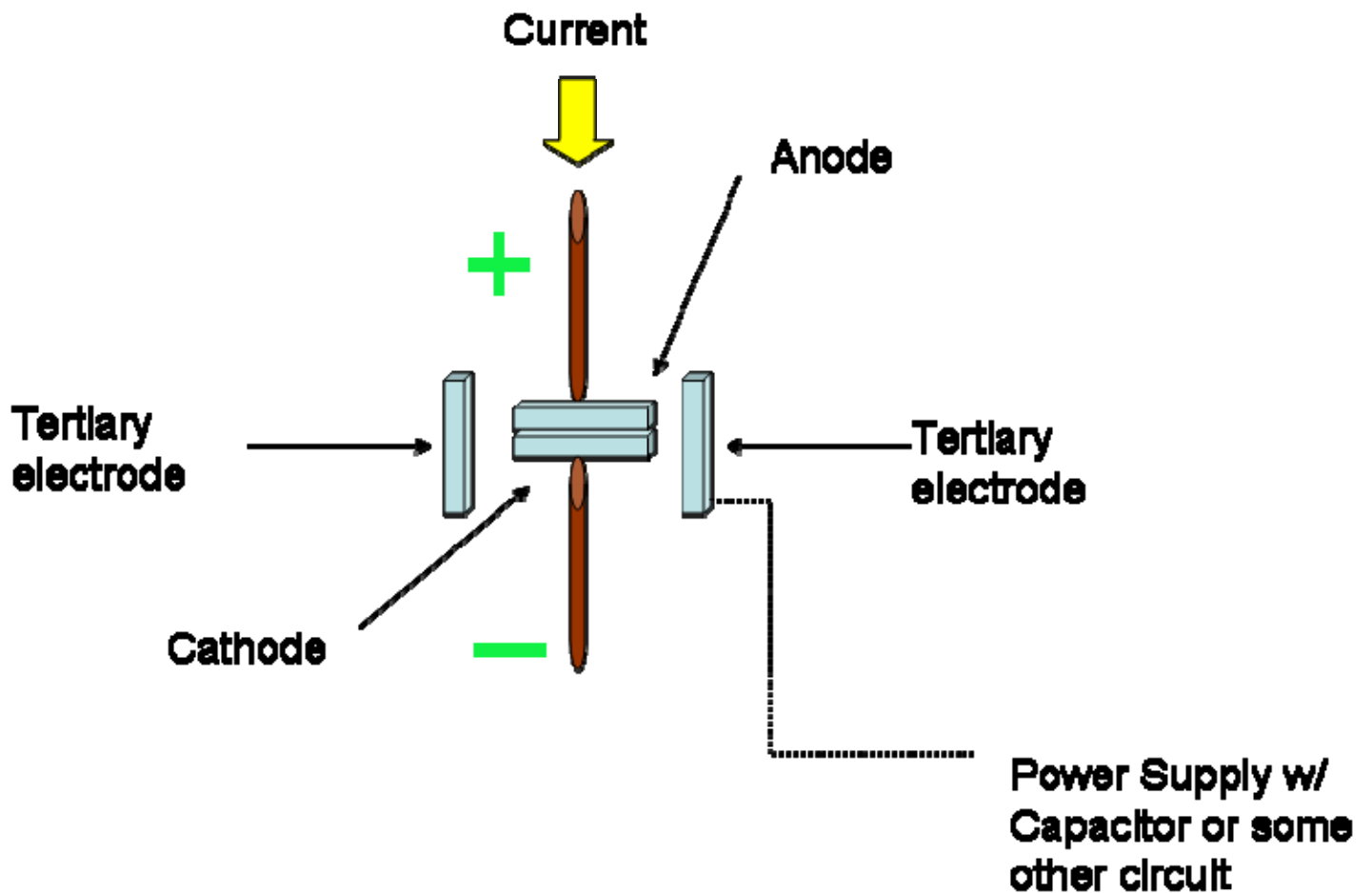


Figure 4. Closed switch. Magnetic field not shown. The tertiary electrode can be connected to ground through a biased capacitor or other circuit.

B. OPENED SWITCH

In this double-pole switch, when the switch is open, the electrons and ions in the plasma between the main cathode and anode will be diverted to a tertiary electrode by an applied magnetic field, thus suppressing the arc and fully opening the switch. The electrons will spiral along the magnetic field lines and ions will be diverted. A simplistic schematic depicting the general principle of operation for this switch is shown in Figure 5.

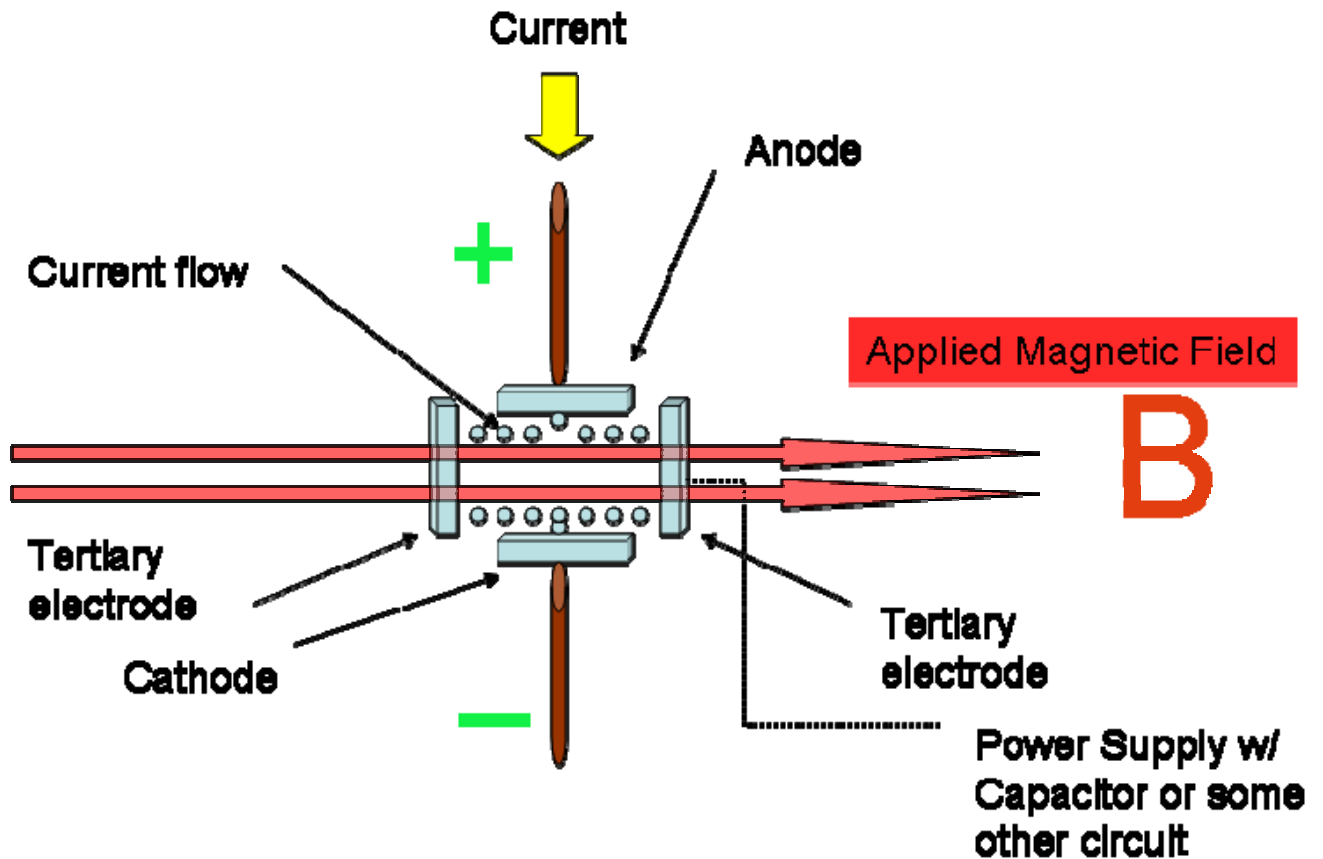


Figure 5. Opened switch.

The figure above is intended to show the concept of operation and not the exact configuration. (A cylindrical switch is shown and discussed in the next section.) If there had been no external magnetic field applied to direct the electrons and ion particles, the arc would remain developed and allow current flow as demonstrated in Figure 6.

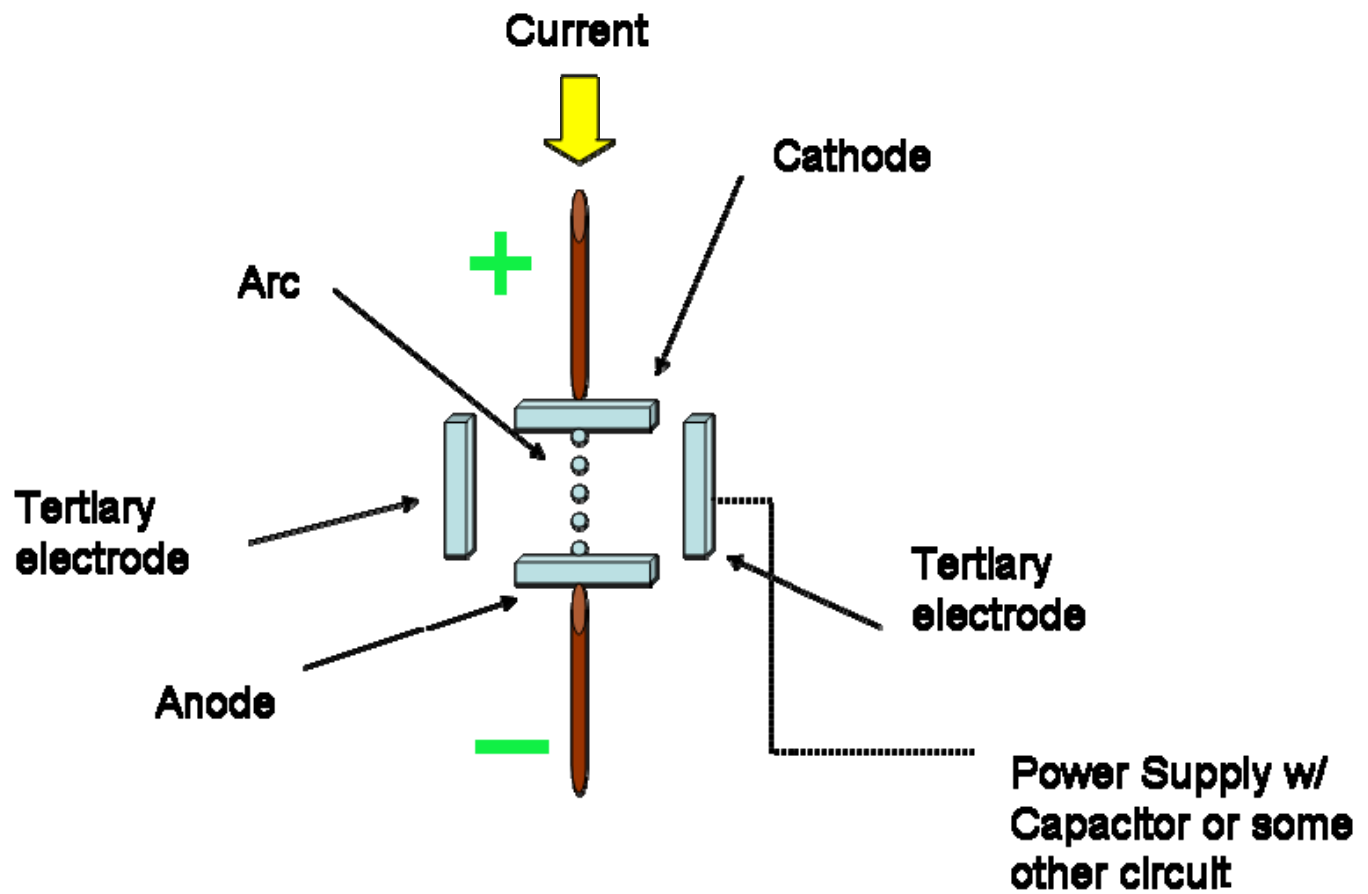


Figure 6. Opened switch without applied magnetic field.

THIS PAGE INTENTIONALLY LEFT BLANK

III. PROTOTYPE SWITCH

A. SWITCH DESIGN

For an initial test of the concept, a switch was designed to fit into one pod of a vacuum ion pump. The external magnet integral to this pod provided a magnetic field perpendicular to the electric field. Figure 7 shows the switch designed to test this concept without its vacuum ion pump encasement and with a cutout of the tertiary electrode for better interior viewing. All detailed drawings can be found in the appendix for each component with specific dimensions.

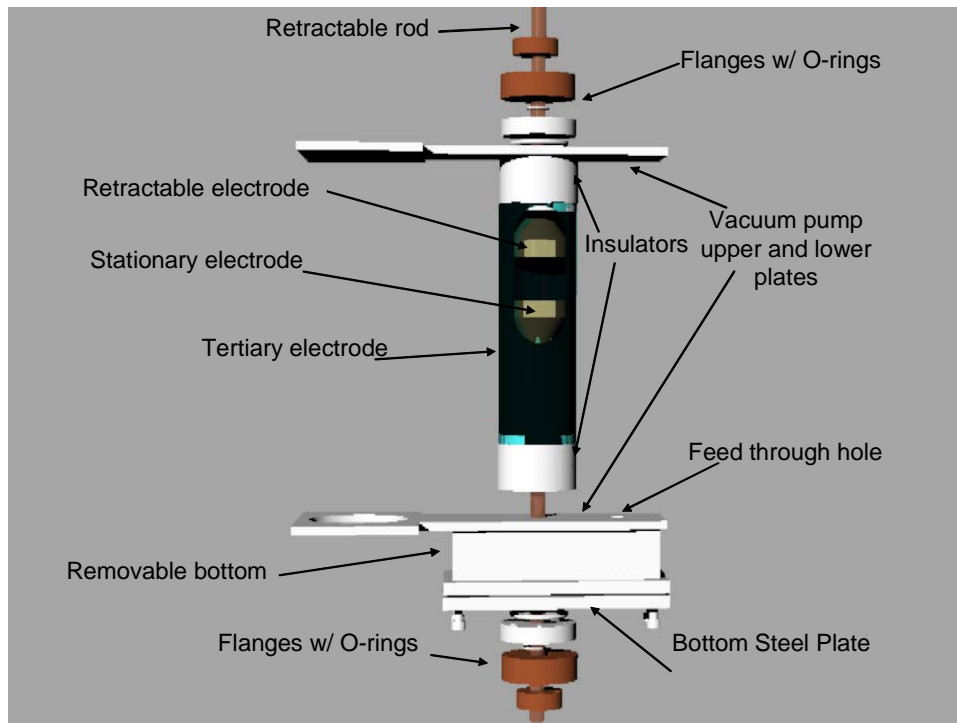


Figure 7. Prototype switch.

The switch is engineered with an upper movable rod to guide and support the retracting copper electrode depicted in a faint yellow color. The bottom electrode is held fixed and is made from copper. Surrounding the two copper electrodes is the cylindrical tertiary electrode as viewed in black; it extends for approximately 4 inches of the vacuum ion pump pod and is screwed into a bottom insulator for support and ease of assembly. The top of the tertiary electrode is also aligned and supported by an insulator sleeve. In

order to assemble the switch, the bottom box steel plate of the vacuum pump plate will be used as a mounting support plate. A feed through hole will allow an ammeter to measure the current being collected at the tertiary electrode during operation and to permit the potential of the electrode to be adjusted. Lastly, the interior vacuum will be maintained by a turbo pump and all removable seals are made with o-rings.

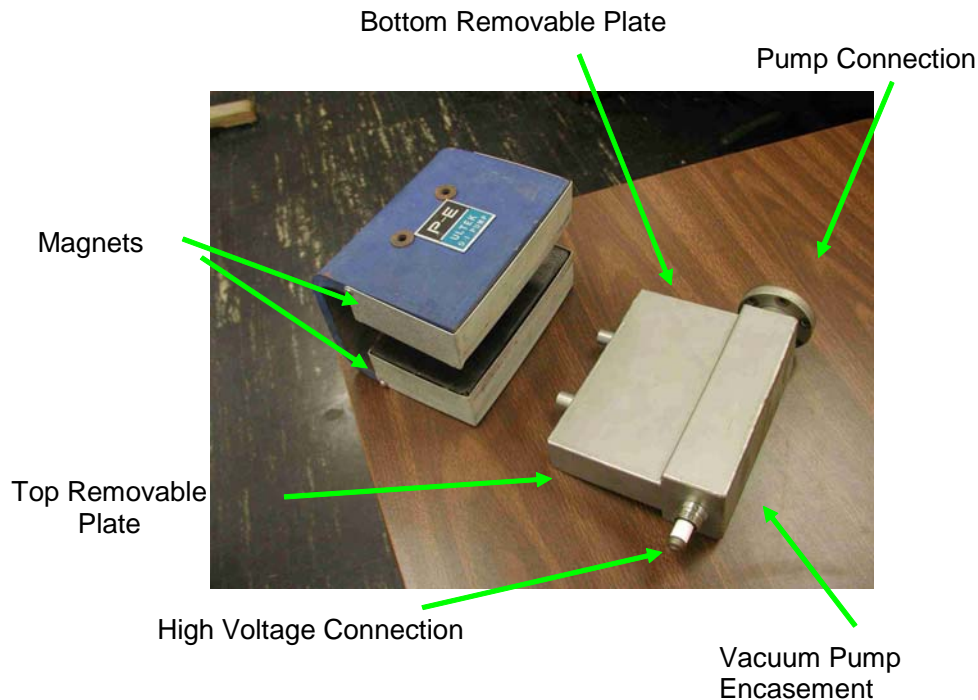


Figure 8. Vacuum ion pump before modification. (The locations of the planned modifications are indicated.)

1. Sputter-Ion Vacuum Pump Housing

Even though this double pole switch design is limited by the vacuum ion diode pump housing, using this structure for the switch housing was a sensible choice because it includes a pump connection to produce a vacuum, a high voltage connection to supply current to the electrodes, a metal shield to provide secondary protection and an established magnetic field from the attached magnets. The vacuum ion pump pod is shown in Figure 8 with its planned modifications to support the switching assembly. The Duniway Stockroom Corporation vacuum sputter-ion pump has an expected magnetic field between 0.10 to 0.20 T within a 3-7 kV high anode voltage range. [6] Using a Hall

probe, the average measured magnetic field was 0.16 T between the blue magnet plates. The inherent magnetic field of this particular vacuum pump may be sufficient, but a larger magnetic field may be needed to deflect the particle trajectories to open the switch properly.

2. FEMLAB Simulations

COMSOL Physics 3.2 (FEMLAB) software was used to calculate single particle trajectories between the two switching electrode plates for a potential difference of 300 V and a magnetic field of 0.16 T. In addition, a grounded cylinder surrounding the main electrodes was the tertiary electrode. Initial velocities were predetermined initial parameters for the electron and copper ion based on expected energies the particles would have within an arcing state. Using these initial conditions, FEMLAB calculated the electric and magnetic field acting on the particles. The spacing and layout were copied exactly from the actual dimensions of the magnet on the vacuum pump and the electrode design for the prototype switch to make the model as realistic as possible. Copper electrode discs were 2 cm apart with a 0.16 T magnetic field strength produced by the 7 inch long magnets. Forces on the particles were calculated by using all the velocity components from the electric and magnetic fields to demonstrate the particle's path as expressed in Eq. (1) below. The mass of the particle is represented by m , \vec{v} is the particle velocity, \vec{E} signifies the electric field between the electrodes, \vec{B} is the magnetic field, t is the time and q is the charge on the particle. FEMLAB is a finite element code that calculates the fields from first principles for the given boundary conditions. Then it evaluates the single particle trajectories based on Eq. (1).

$$m \frac{d\vec{v}}{dt} = q(\vec{E} + \vec{v} \times \vec{B}) \quad (1)$$

a. Electron Trajectory

In Figures 9 and 10, the electron's trajectory is shown as a helical spiral with an initial position near the ground electrode with an initial velocity of 10^6 m/s (corresponding to 2.8 eV) along the copper rod direction. The force imparted on the electron is represented by different colors on a linear scale; red for stronger forces and blue for weaker forces. The maximum force calculated was -2.02×10^{-16} N while the

minimum force was -2.13×10^{-16} N. The electron does not arrive at the tertiary electrode shown in Figure 10. With these initial conditions, the electron does not reach the anode, suggesting that there will be a disruption in current flow and the overall double pole switch concept could be achieved.

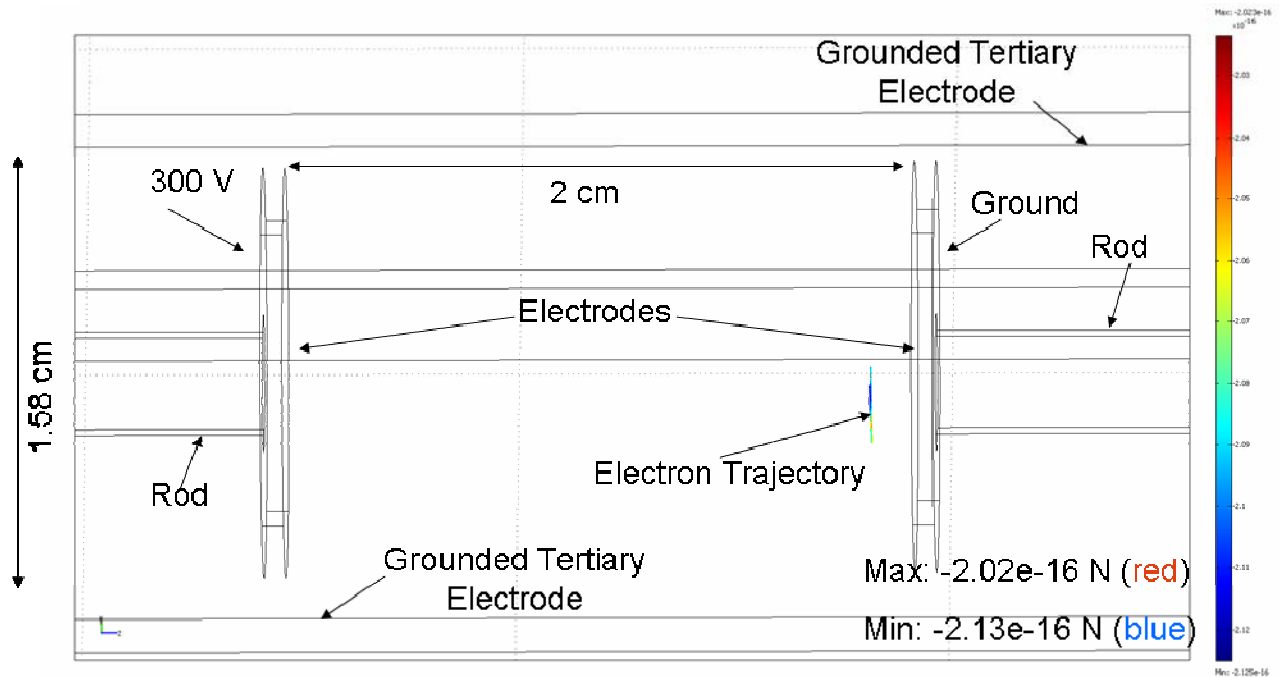


Figure 9. Side view of electron trajectory within the cylindrically symmetric switch. Transparent view. (Some extraneous lines used by FEMLAB are shown but have no affect on the results.) Important components are labeled.

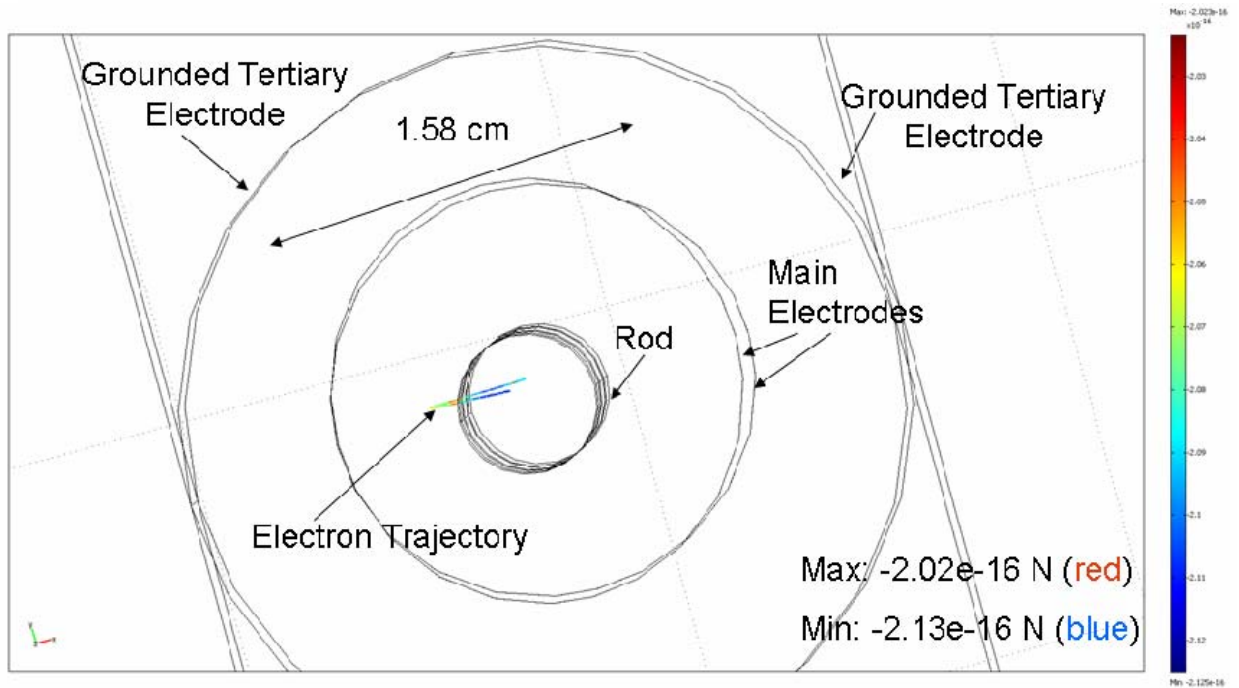


Figure 10. Electron trajectory looking from the retractable rod perspective; slightly off axis. (Some extraneous lines used by FEMLAB are shown but have no affect on the results.) Important components are labeled.

b. Copper Ion Trajectory

Since ionic particles will be ejected from the copper electrodes within the switch, the copper ion's motion was also examined. The mass of a singly ionized Cu atom (Cu^+) was taken to be 63 amu. The initial velocity of Cu^+ was taken to be 350 m/s, corresponding to an energy of 0.040 eV for each simulation. The copper ion's trajectory paths are demonstrated in Figures 11, 12 and 13 where the paths are slightly curved, not resembling the electron's helical shaped trajectory. It is apparent that the magnetic field has less influence on the heavier copper ion's motion than it did on the motion of the electron. These three different trajectories show that a small change in initial position greatly affects the probability of the charged particle being captured by the tertiary electrode or being diverted away from the main cathode-anode path. Thus, magnetic fields larger than 0.16 T may be necessary to divert larger ion particles and prevent Cu^+ from traveling from the anode to the cathode.

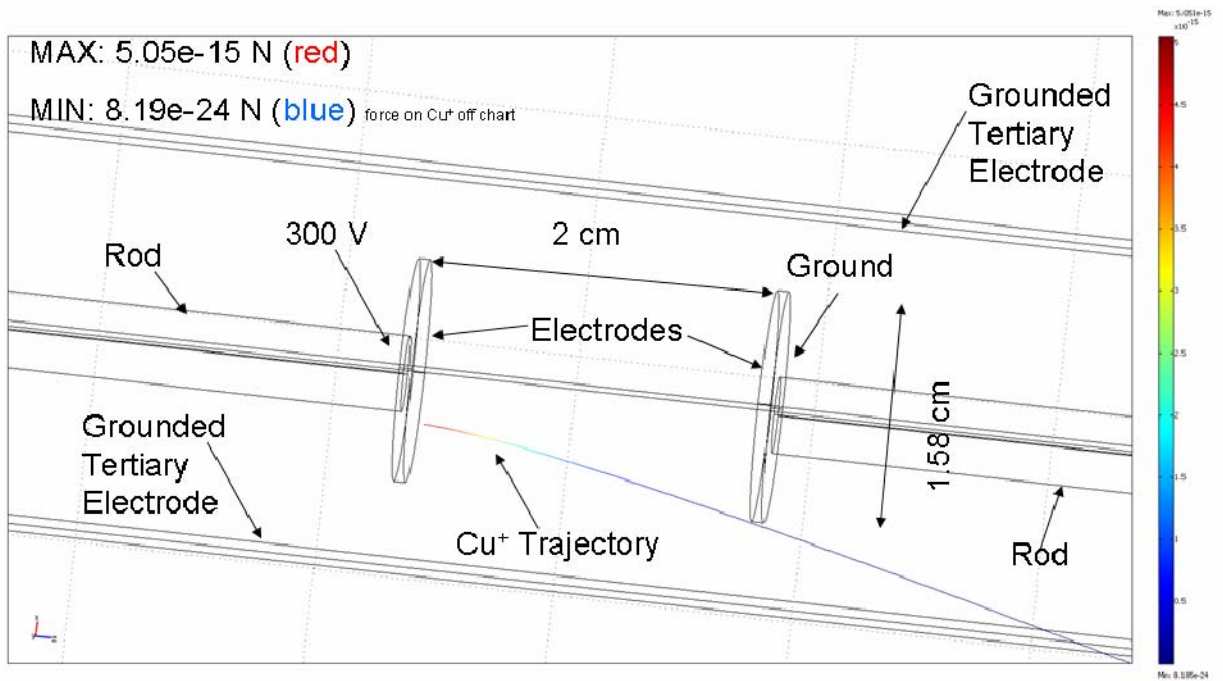


Figure 11. Side view of copper ion trajectory starting near bottom of anode within the cylindrically symmetric switch. (Some extraneous lines used by FEMLAB are shown but have no effect on the results.) Important components are labeled.

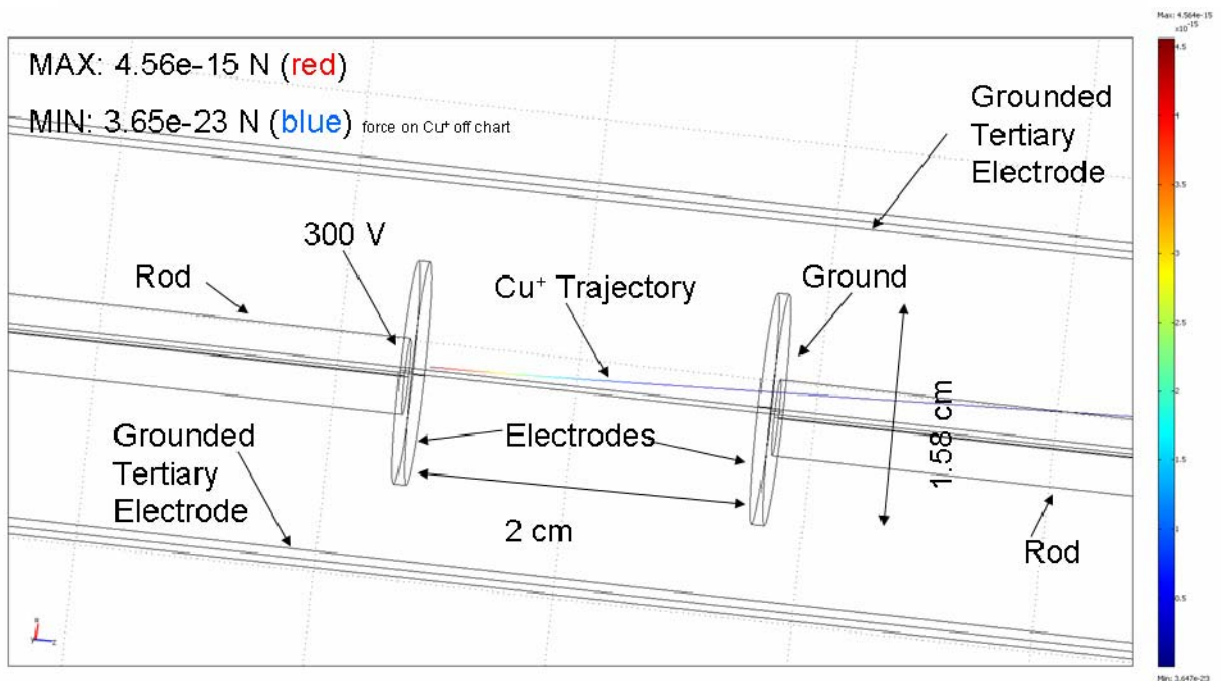


Figure 12. Side view of copper ion trajectory starting near middle of anode within the cylindrically symmetric switch. (Some extraneous lines used by FEMLAB are shown but have no effect on the results.) Important components are labeled.

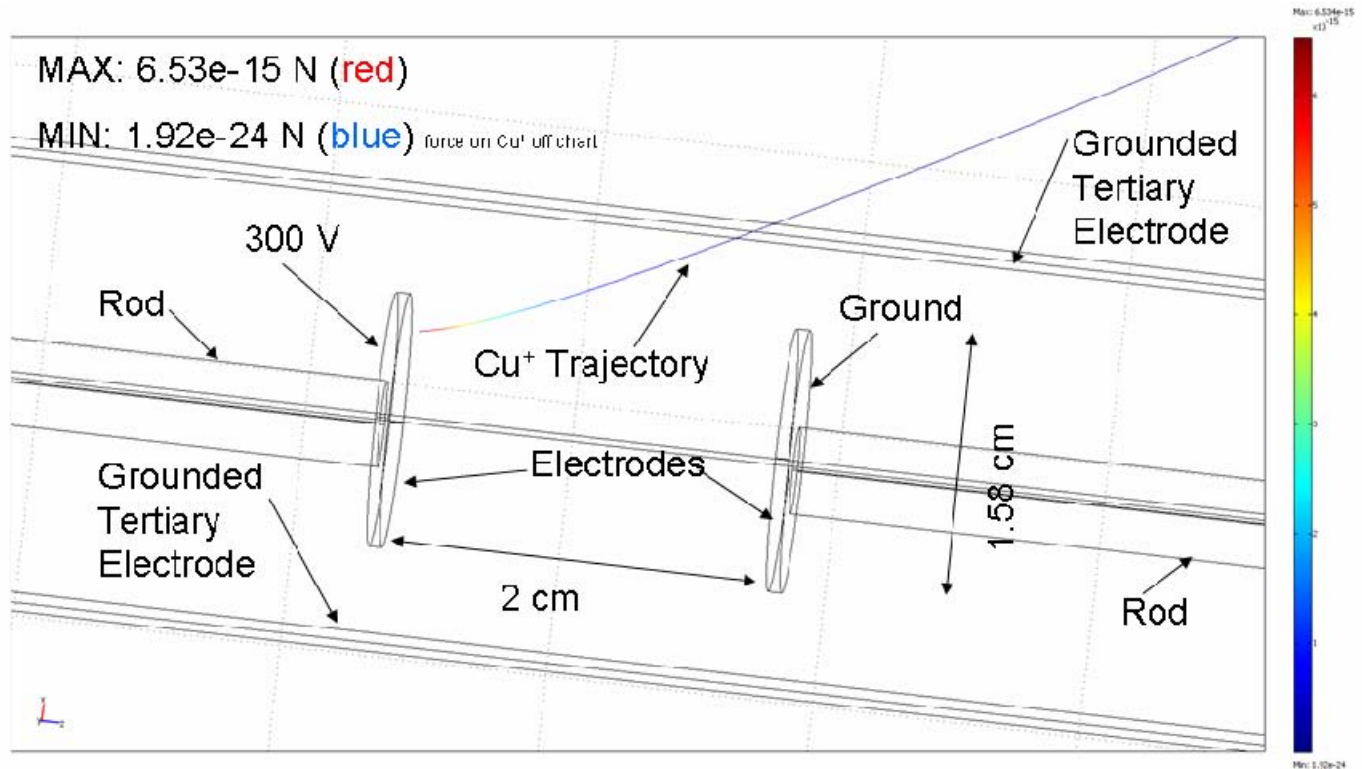


Figure 13. Side view of copper ion trajectory starting near top of anode within the cylindrically symmetric switch. (Some extraneous lines used by FEMLAB are shown but have no effect on the results.) Important components are labeled.

The simulations also showed that electric field strength varied greatly along the main path between main anode and cathode. Figures 14, 15 and 16, show the electric field strength measured near the anode, midway between the two main electrodes, and lastly near the cathode. The lack of symmetry shown in the electric field strength across the grounded outer cylinder is due to the numerical error of the linear solver used in the 3-D simulation. The variation of the electric field in Figures 14-16 occurs because the cathode sits within the grounded outer electrode, i.e., it's the "bottom" of a grounded can. The electric field will be larger where the anode is near the grounded tertiary electrode and small near the "bottom" of the can.

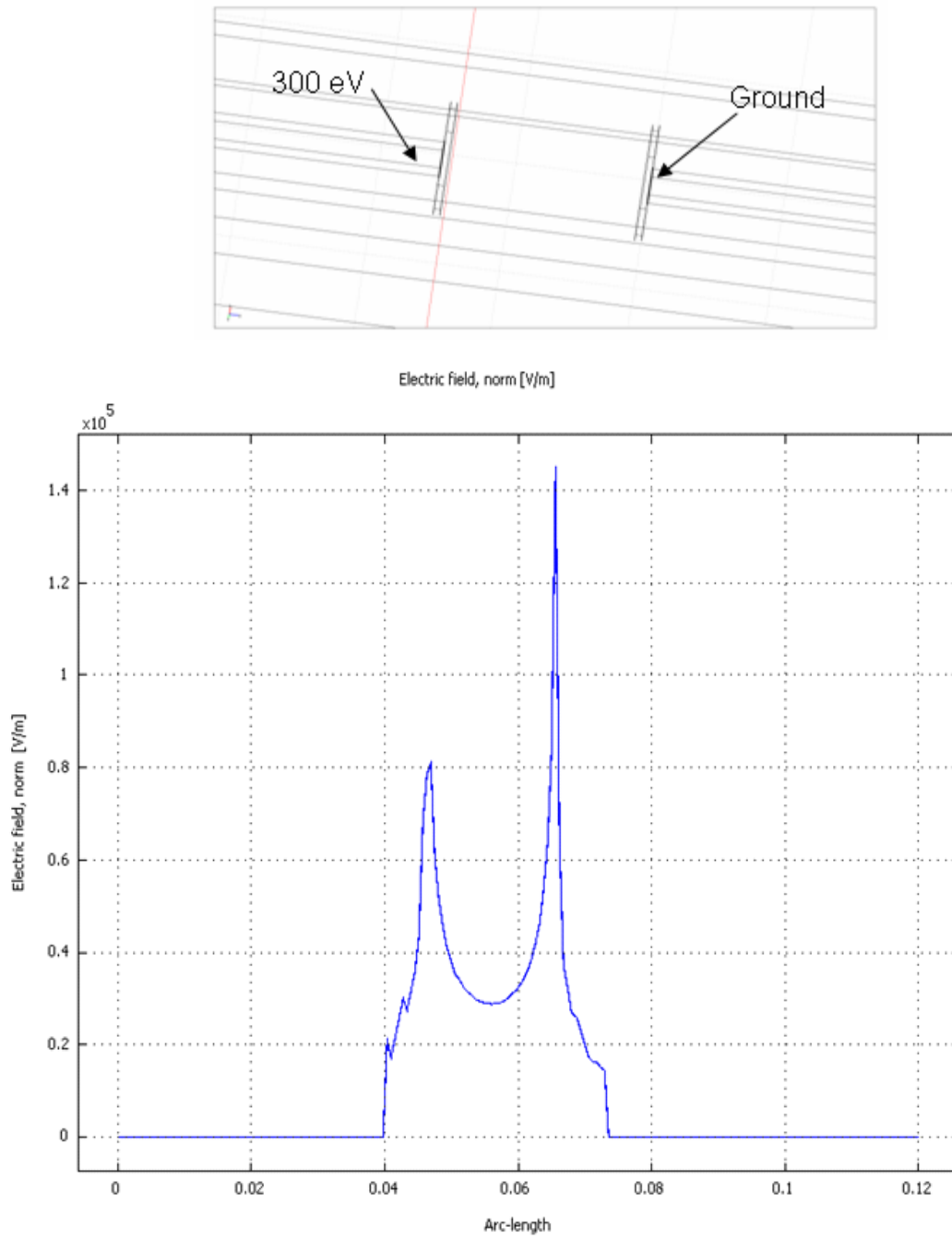


Figure 14. Electric field strength along red line near anode.

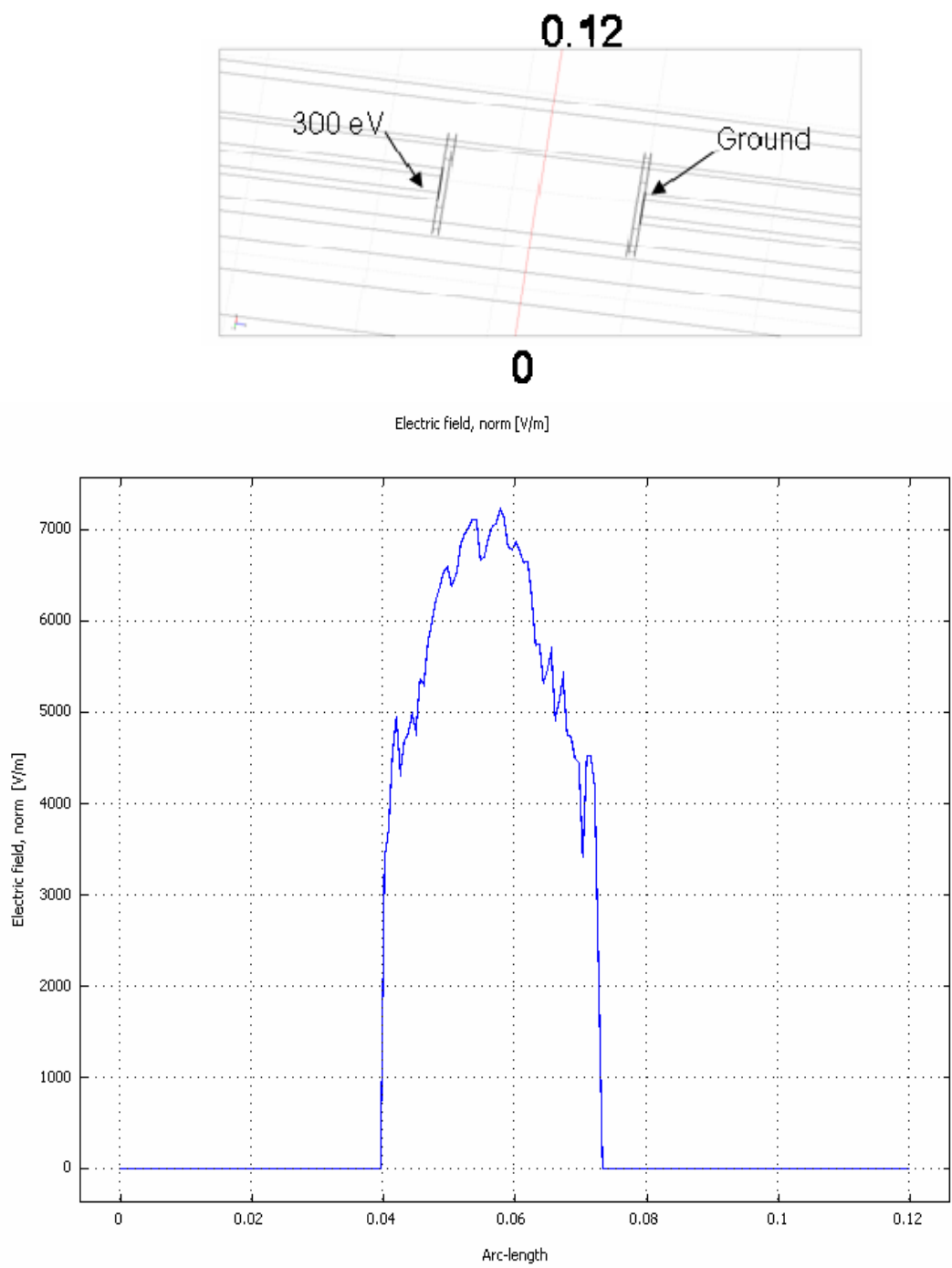


Figure 15. Electric field strength along red line midway between main electrodes.

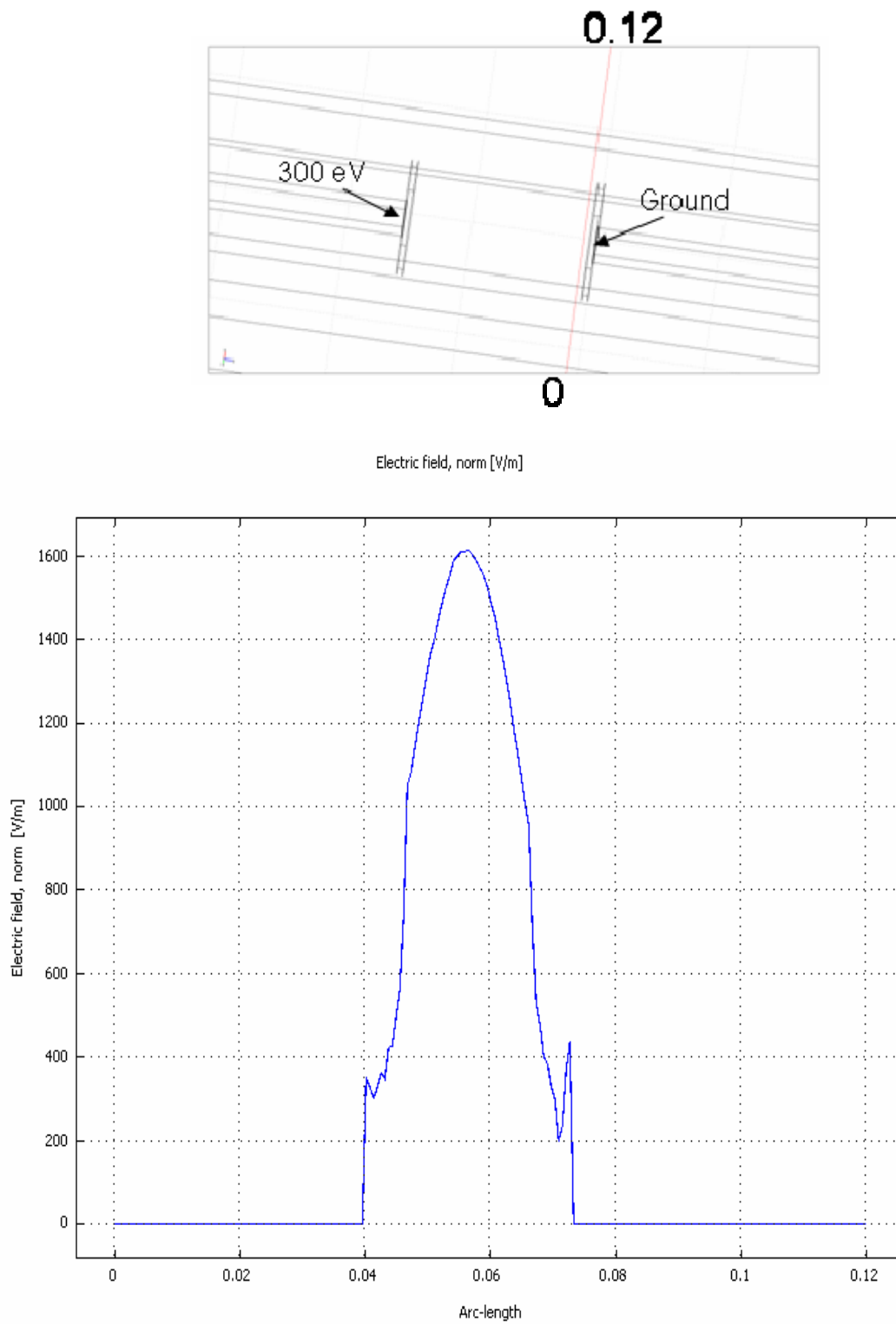


Figure 16. Electric field strength along red line near cathode.

From the depictions above, it is shown that initial position and electric field strength impact Cu^{++} 's path. More analysis will need to be conducted to better understand how a larger magnetic field strength will deflect the charged particle from the cathode.

B. SWITCH ACTIVATION

A mechanism was needed to retract the movable electrode 1 cm in 1 ms in order to best simulate the timing constraints of the switch. My first activation design involved a fork shaped slipping handle to contain a 234 lbs force from a compression spring as viewed in Figure 17. The purpose of this device was to verify the mechanical and timing properties of the spring initiated assembly.

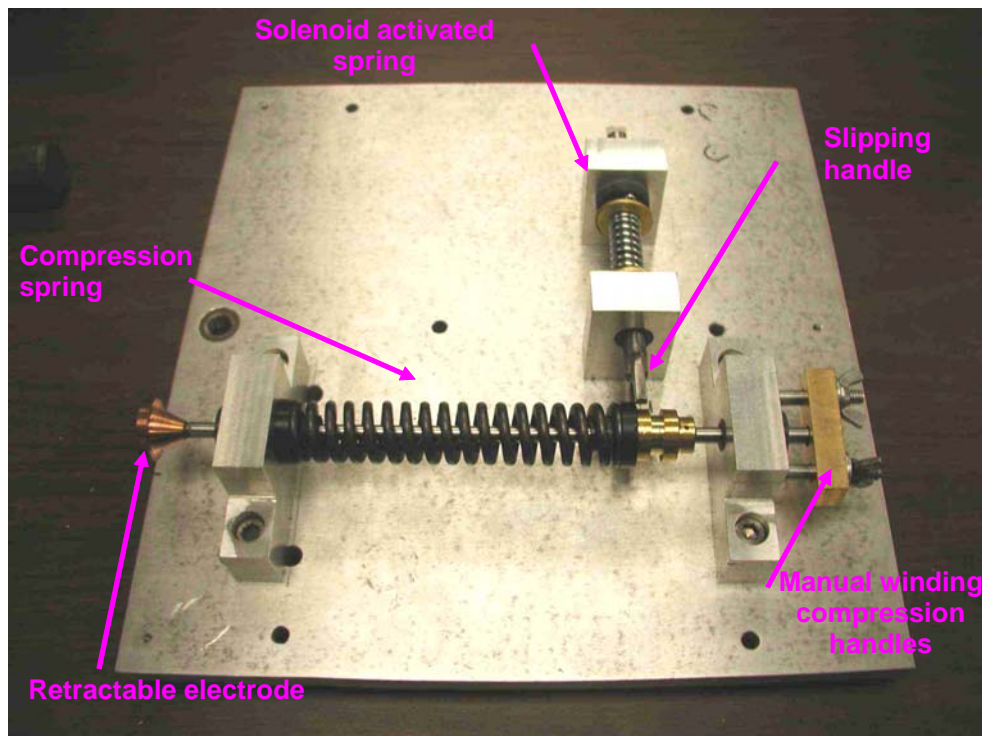


Figure 17. Spring activation assembly.

The manual winding handles shown in Figure 17 effortlessly compressed the five inch stainless steel spring 1 cm to engage the slipping handle on the main spring. A solenoid activated the auxiliary spring on demand and pulled the slipping handle off the main compression spring. Once the compression spring expanded, the electrode was

released and let travel. This device proved to be unreliable because the slipping handle would get canted and lodged as a result of the excessive forces combined with the retarded retraction of the slipping handle.

In order to make a viable initiating device, a design should resemble the triggering mechanism of a firearm so that relieving a little pressure will provide a huge release of force. This objective can be accomplished by having the force taken by the pivot as demonstrated below in Figure 18.

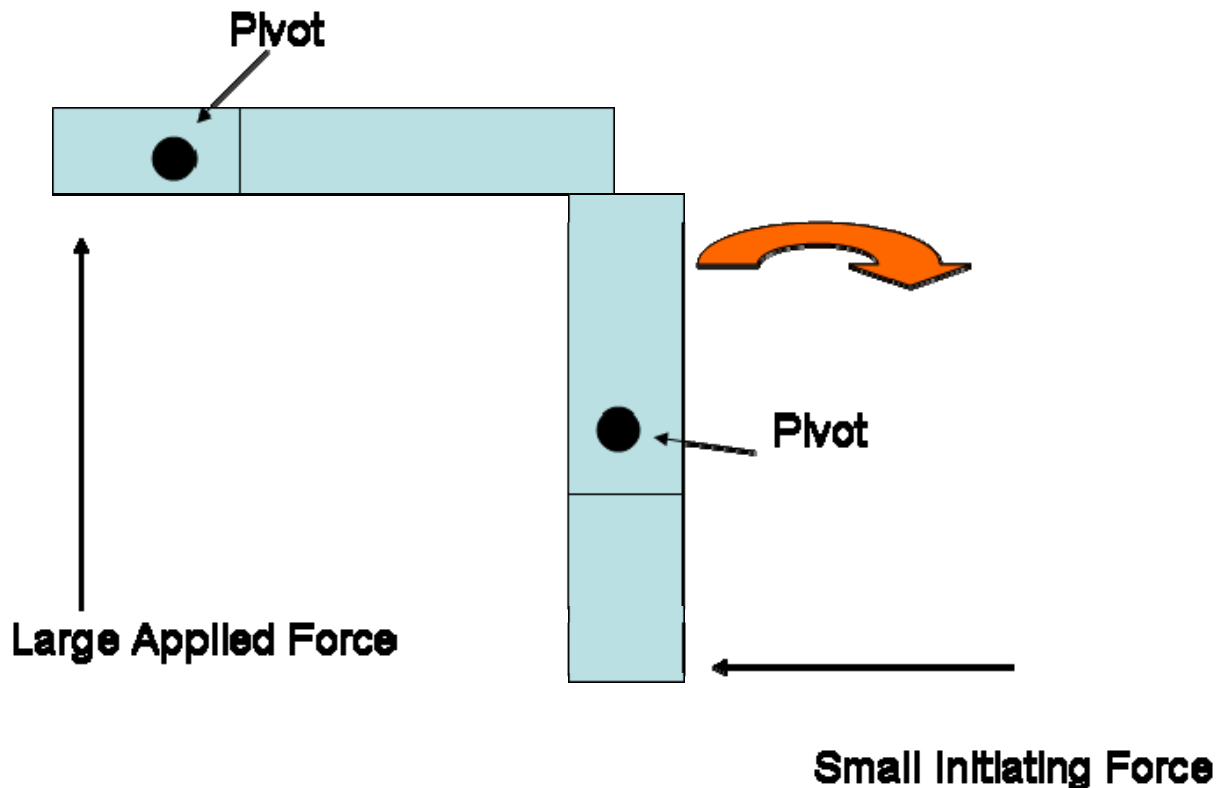


Figure 18. Suggested triggering mechanism.

1. Hand Calculation of Necessary Force to Retract the Electrode

Although the spring force initiating device did not perform adequately, the estimation to compute the required force to move the electrode 1 cm in 1 ms is pertinent information for the prototype switch. The copper rods were 0.25" in diameter with a predetermined length of 4" while the copper tungsten electrodes were 0.625" in diameter and 0.25" thick. The estimated force required to move one set (since the bottom electrode and rod would be fixed) could be computed. The densities of copper and

copper tungsten are 9 g/cc and 12.52 g/cc respectively. The total mass of one electrode disc and rod was 46.6 g. We assumed that the initial position and velocity of the retractable electrode were zero. From these dimensions and properties, and $x = \frac{at^2}{2}$, the force was calculated using

$$F = \frac{2mx}{t^2} \quad (2)$$

where F represents the force, m is the total mass of the electrode and rod, x is the distance of electrode travel ($x = 1$ cm) and t is duration of travel ($t = 1$ ms). Consequently, the required force was found to be 203 lbs force or 892 N.

C. SWITCH TEST CONCEPT

1. Component Design Considerations

P-Spice software was used to examine the switch's functionality and electric properties within the PFIN circuitry to provide power to the railgun. As displayed in Figure 19, SW1 is the prototype switch of interest to test for opening. Four SAFT VL8V (4.1 V, 1 mΩ resistance) batteries were assembled with two of them in series and in parallel with the other set of two to supply a total of 8.2 V across the circuit and a resistance of 1 mΩ. Their arrangement was chosen to minimize circuit resistance to decrease heating losses. More batteries could have been arranged in other better configurations, but I was limited by battery availability. The PFIN circuit is shown schematically in Figure 19.

a. Inductor Design Specifics

A solenoid coil of diameter 0.6 m and length, $\ell = 0.5$ m, was chosen for the inductor. The inductor size was selected because of its sufficient diameter to envelope the vacuum ion pump housing for future additional magnetic field strength. For a 0000 cable, the resistance/length, R_ℓ , is approximately 1.6×10^{-4} Ω/m. The length of one cable is $l \approx 2\pi rN$ where l is cable length, r is the radius of the solenoid and N is the number of turns. Since we already have an inductor made in the lab, we know it has about 50 μH inductance (see appendix C), 0.3 meter radius and $N = 9$. Therefore, the length of cable is 17 meters long. For n parallel strands of wire, the resistance of the coil

would approximately be $R_{coil} \approx 2\pi r R_t \frac{N}{n}$. We intend to use five parallel strands for a total resistance/five strands is $5.42 \times 10^{-4} \Omega$. Referring to the circuit in Figure 19, I anticipate that the battery could drive a maximum current, $I \approx \frac{V_1}{R_2 + R_3} \approx \frac{8.2V}{1.54 \times 10^{-3} \Omega} \approx 5.3 \text{ kA}$, through the inductor. The maximum energy stored in the inductor would then be 708 J and the maximum magnetic field in the inductor would be approximately 0.120 T.

2. P-Spice Simulation and Analysis

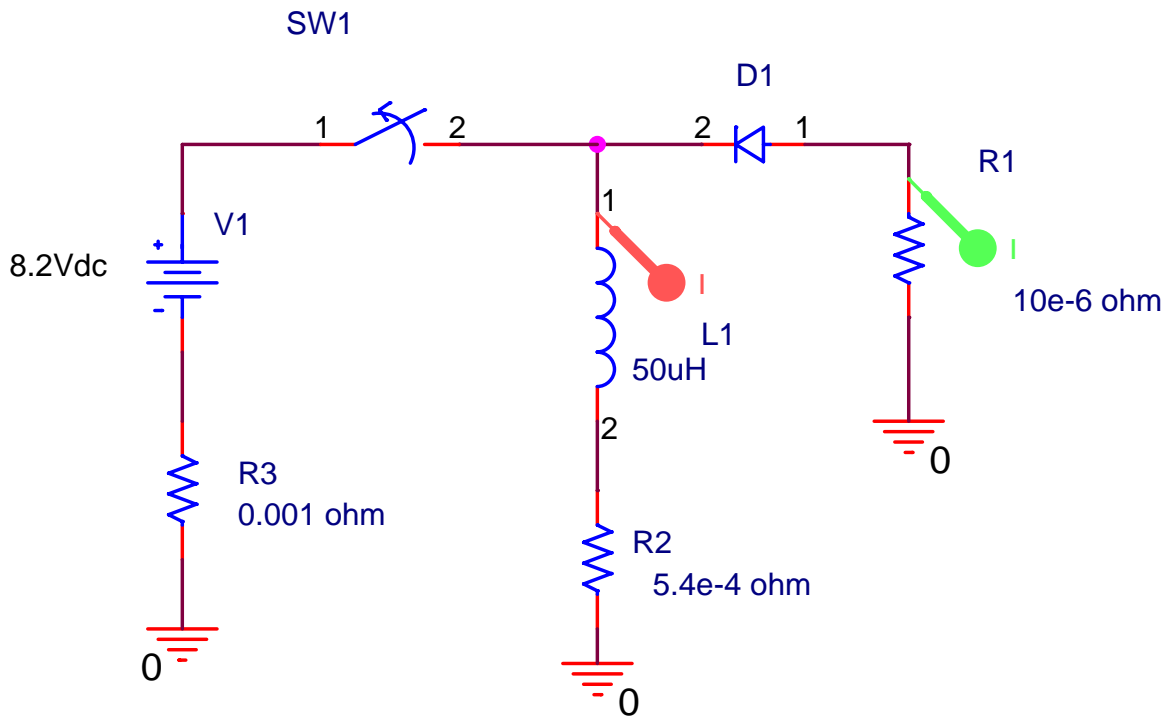


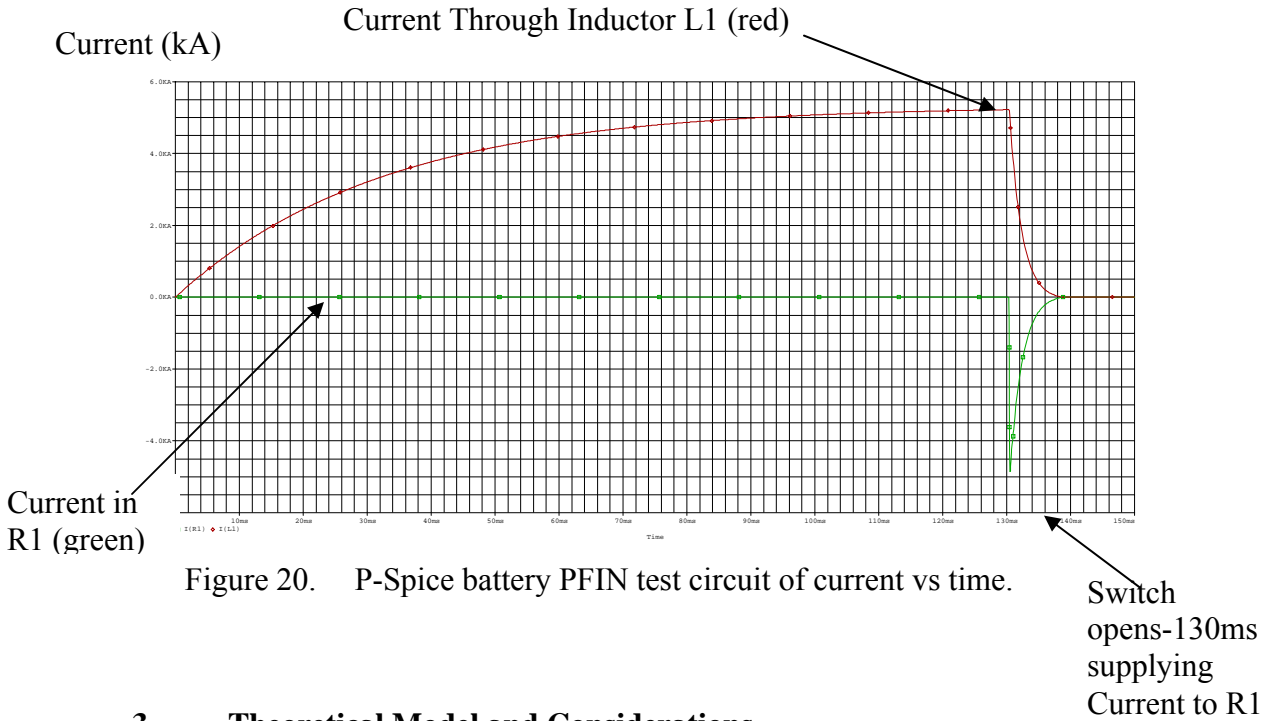
Figure 19. P-Spice railgun battery PFIN test circuit.

a. SW1 Switch Analysis for Closed Circuit

The low-voltage battery energy is stored in the inductor, L1, as magnetic field energy. The red current probe in Figure 19 gives the current flow shown in Figure 20 by a red colored line. The green current probe monitors railgun current depicted by the green curve in Figure 20. Current in the inductor will rise until switch SW1 is opened. SW1 opens 130 ms after it closes.

b. SW1 Switch Analysis for Opened Circuit

SW1 is closed then opened 130 ms later, and the inductor's magnetic field induces current flow through load resistance R1, the railgun, while a generic diode, D1, prevents any back current flow. The current rises to approximately 5.3 kA as shown in Figure 20. Any inductance in the portion of the circuit containing the battery may produce a high voltage when SW1 is opened, but in this simulation this inductance is set to zero.



3. Theoretical Model and Considerations

Power transferred to the inductor from the battery is conducted in the same manner as a capacitor PFIN assembly, except that there is no instance when the battery's energy is zero. Current flow continues to be supplied by the battery, and battery voltage never reaches zero. The current, $I(t)$, through the inductor and the fractional energy, $\frac{W_L}{W_B}$, is discussed below, where (W_L) represents the energy supplied by the battery and (W_B) signifies the energy supplied by the battery.

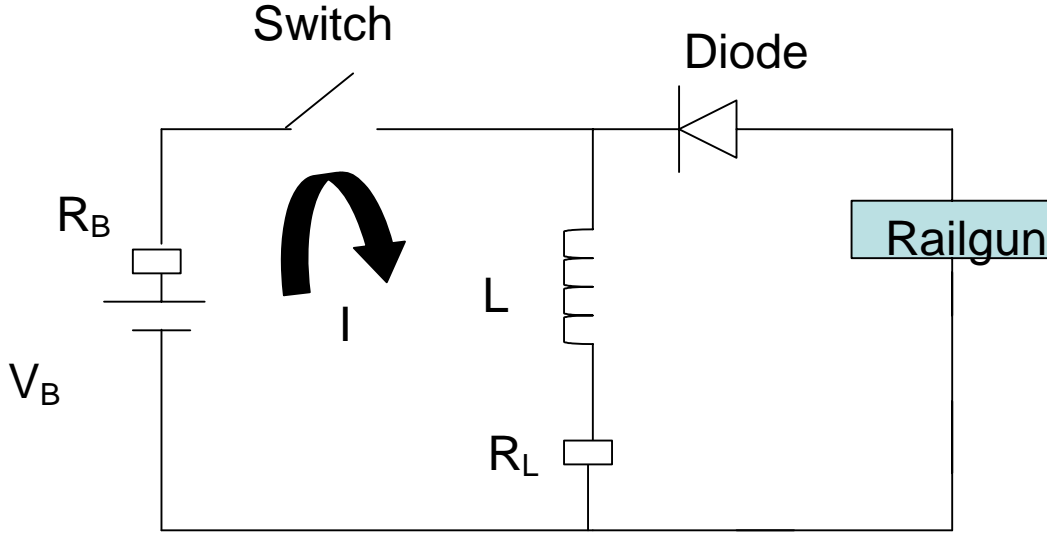


Figure 21. Theoretical railgun battery PFIN schematic.

Referring to Figure 21 for circuit components, V_B describes the battery voltage, R_B is the inherent battery resistance, L signifies the inductor, and R_L corresponds to the inductor's internal resistance. R denotes the total resistance of the battery and inductor.

$$R = R_B + R_L \quad (3)$$

Let τ be a dimensionless time variable expressed by

$$\tau = \left(\frac{R}{L}\right)t \quad (4)$$

The current, I , is given by

$$I = \left(\frac{V_B}{R}\right)(1 - e^{-\tau}) \quad (5)$$

Energy stored in the inductor can be expressed as

$$W_L = \frac{1}{2}LI^2 = \frac{L}{2}\left(\frac{V_B}{R}\right)^2(1 - e^{-\tau})^2 \quad (6)$$

The energy supplied by the battery is

$$W_B = V_B \int Idt = L\left(\frac{V_B}{R}\right)^2 (\tau + e^{-\tau} - 1) \quad (7)$$

Examination of Figures 22 and 23 shows that a lot of energy is lost as dissipative heat. At a dimensionless time of approximately $\tau = 4$, current approaches about 97% the maximum possible, $\left(\frac{V_B}{R}\right)$. For parameters and conditions given in Figure 19, $\tau = 4$ was chosen, and the corresponding time of 0.13 seconds was determined from Eq. (7). Figure 23 indicates that when switch SW1 opens, approximately 85% of W_B has been lost as heat. In reality a balance must be achieved in regards to opening the switch at a high enough current, but not so high as to damage the switch components or lose too much energy as heat. For this prototype switch test simulation, verifying the operation of the switch opening at extreme current levels would give us reason to believe that it would also function properly at regular railgun operating conditions.

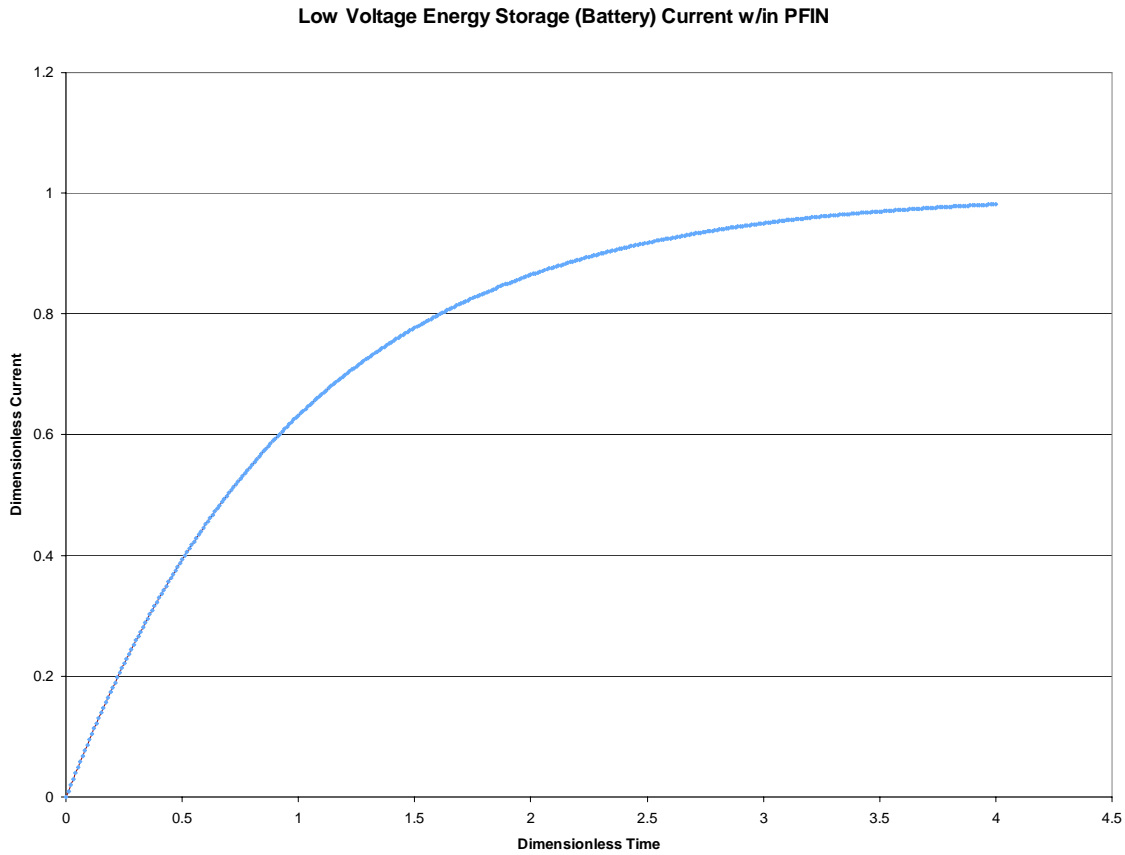


Figure 22. Dimensionless current, $\frac{I}{\left(\frac{V_B}{R}\right)}$, versus dimensionless time, $\frac{R}{L}t$

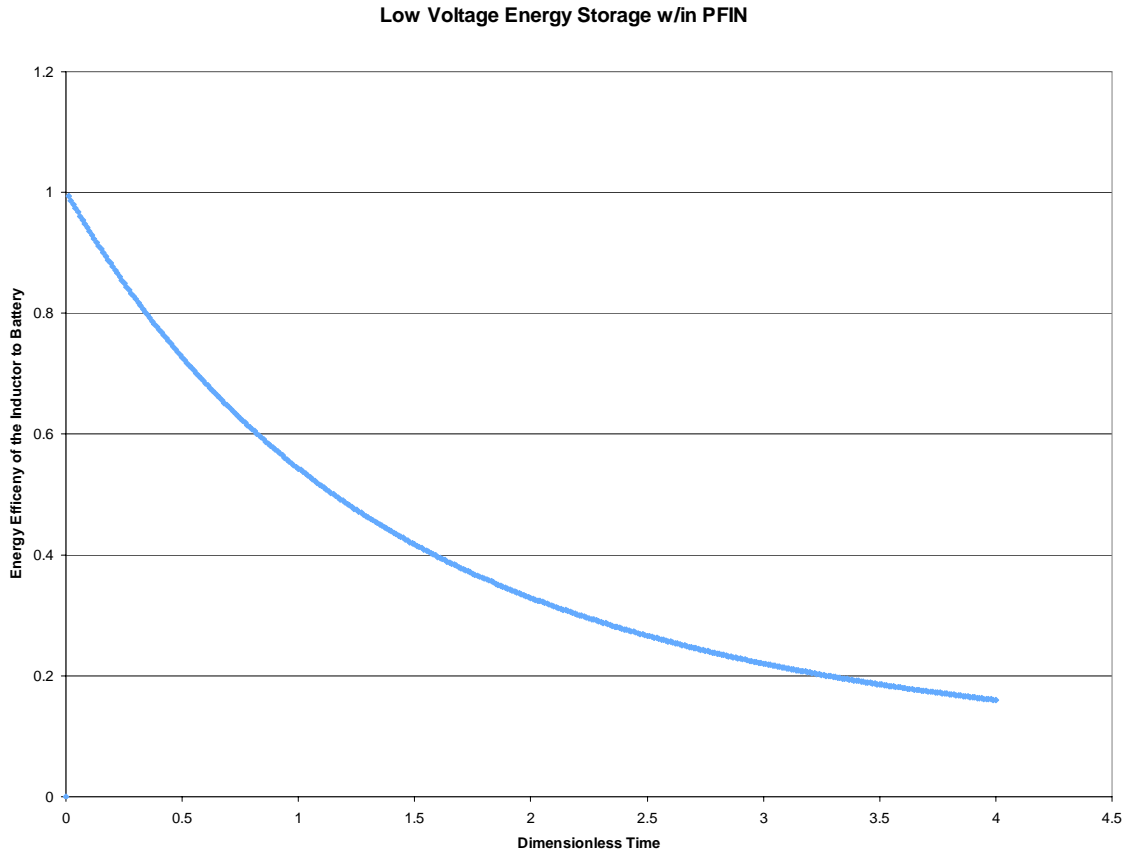


Figure 23. Ratio of inductor energy to battery energy, $\frac{W_L}{W_B}$, versus dimensionless time,

$$\frac{R}{L}t$$

IV. CONCLUSION

We have introduced a new double pole switch concept that may be suitable for high current and high voltage applications, but specifically to provide power to the railgun. A patent proposal was prepared for submission reflecting this new switching idea. In addition, we designed and illustrated an prototype switch to facilitate testing of the double pole magnetic field switching concept. Trajectories computed for Cu^+ and electrons in this switch for $B = 0.16 \text{ T}$ suggest that larger magnetic fluxes may be required to divert current to the tertiary electrode. It was demonstrated that springs can be used to actuate the prototype switch with a suitable triggering mechanism.

THIS PAGE INTENTIONALLY LEFT BLANK

V. FUTURE WORK

The double pole high current high voltage switch construction needs to be assembled as per the technical drawings found in the appendix. The switch assembly can then be tested for mechanical and electrical properties. A new triggering apparatus for switch initiation must be designed and assembled and current measurements between the anode and the tertiary electrode must be made to confirm proper current diversion. If $B = 0.16$ T suffices to extinguish the arc between the two electrodes quickly, then no additional applied magnetic field will be necessary to divert charged particulate matter. If there is poor current interruption due to insufficient magnetic field strength, it will be necessary to increase the magnetic field strength and make new observations. Another option to enhance current interruption within the switch would be to set a low or negative potential at the tertiary electrode to capture ions. This condition, perhaps together with an increased external magnetic field strength, may greatly improve switch operation and needs to be examined.

THIS PAGE INTENTIONALLY LEFT BLANK

APPENDIX A. ASSEMBLY DRAWINGS (O-RING GROOVES, THREADS AND SOME BOLT HOLES ARE OMITTED)

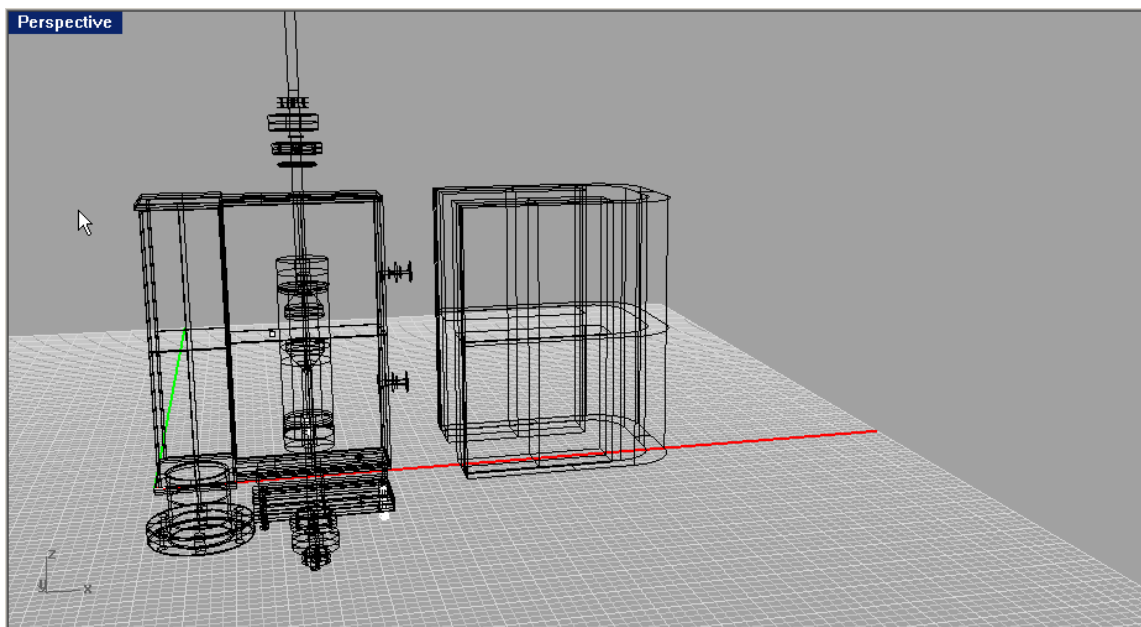


Figure 24. Prototype switch w/ vacuum ion pump pod and magnetic plates.

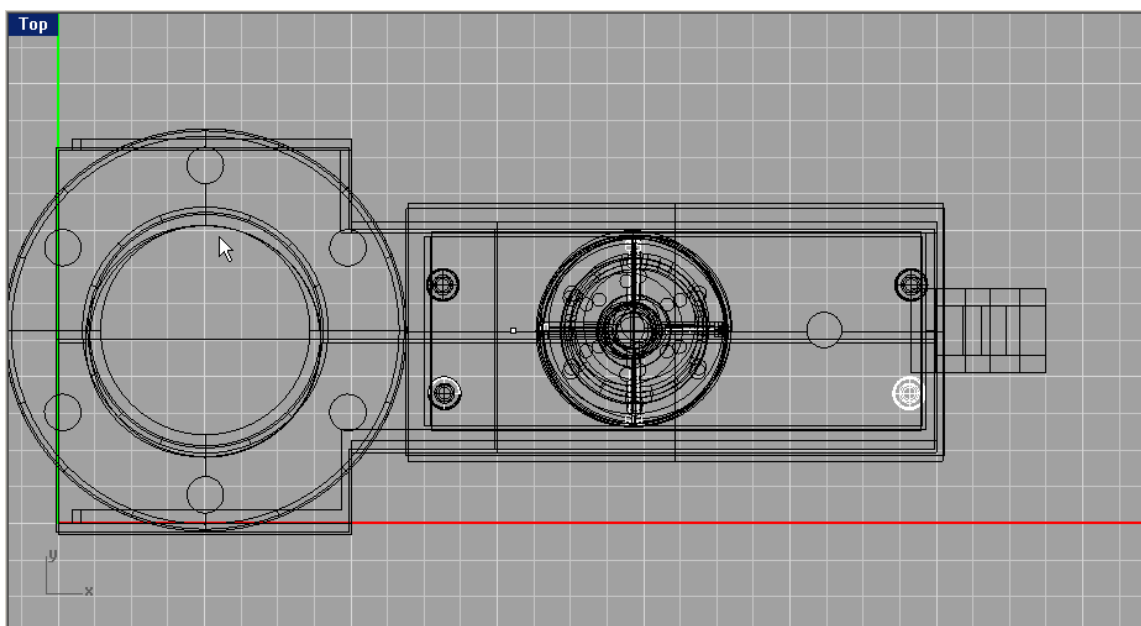


Figure 25. Top view of prototype switch w/ vacuum ion pump pod and w/out magnetic plates.

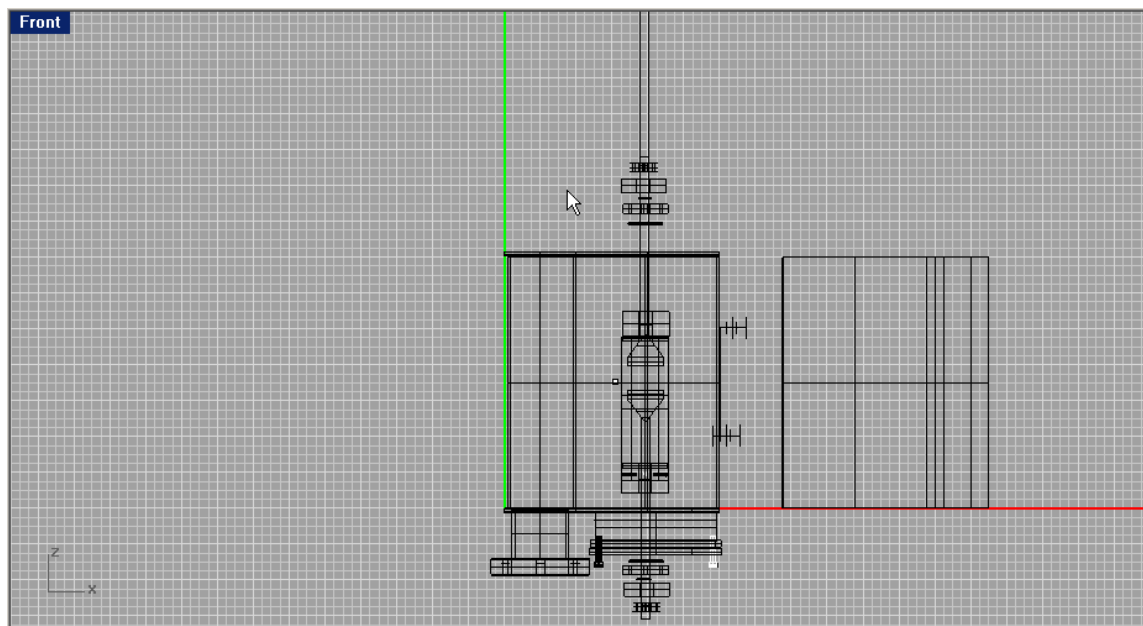


Figure 26. Front view of prototype switch w/ vacuum ion pump pod and magnetic plates.

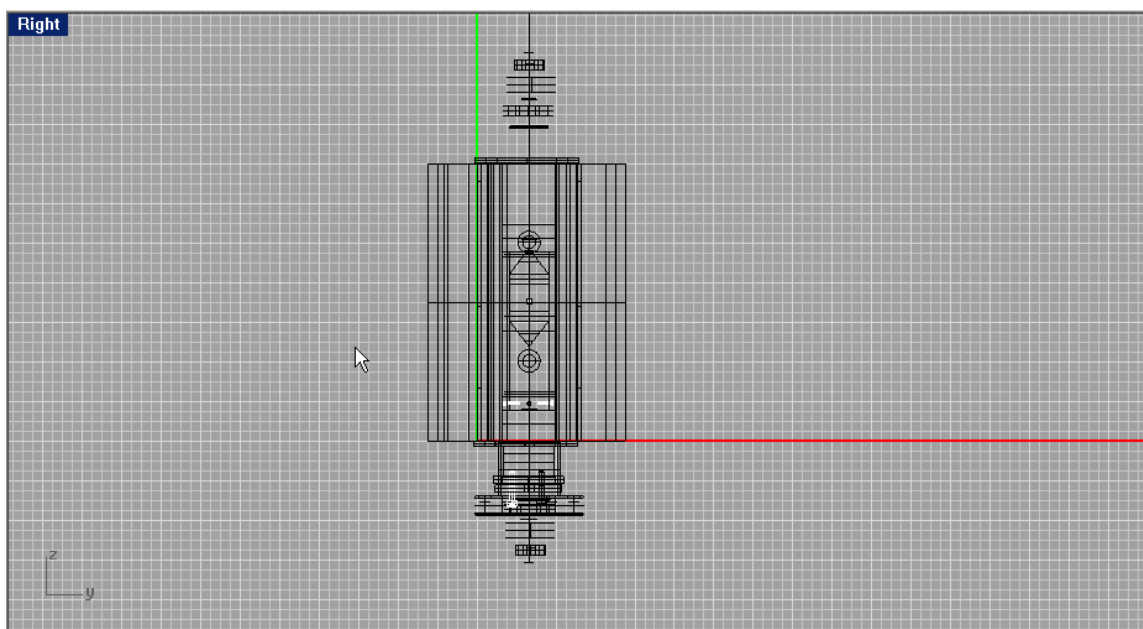


Figure 27. Right view of prototype switch w/ vacuum ion pump pod and magnetic plates.
(Some vertical lines are distorted in the side view due to the drawing program.)

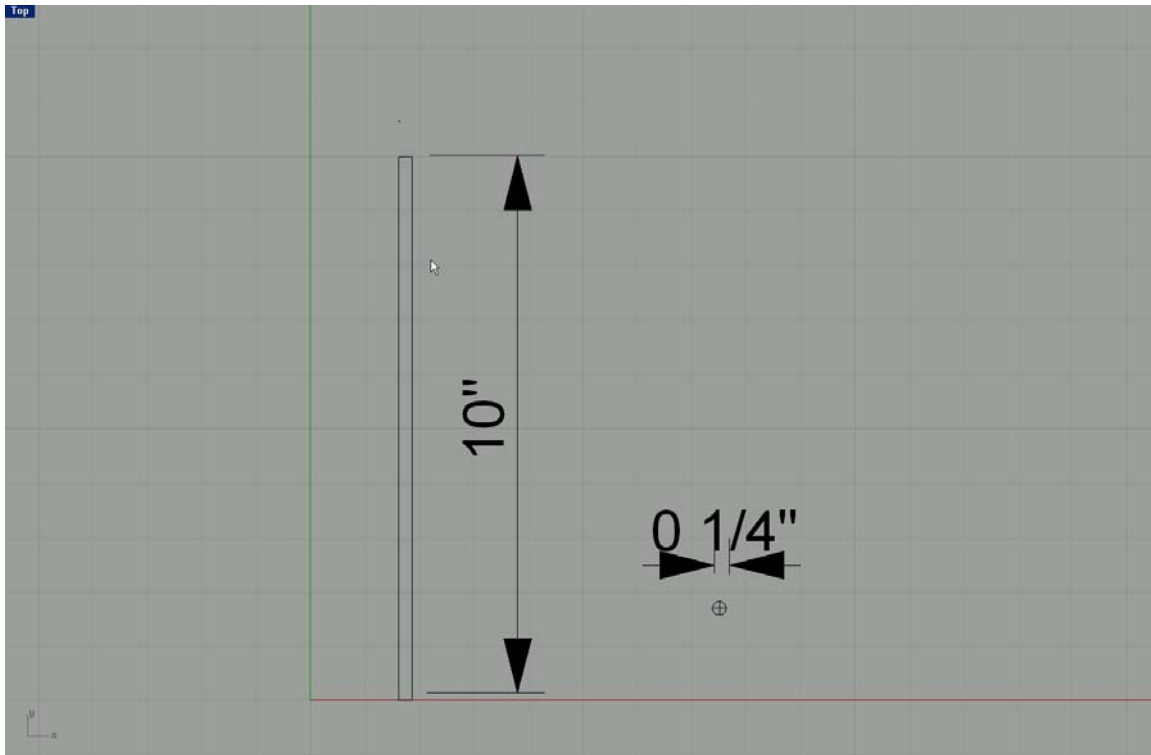


Figure 28. Retractable rod.

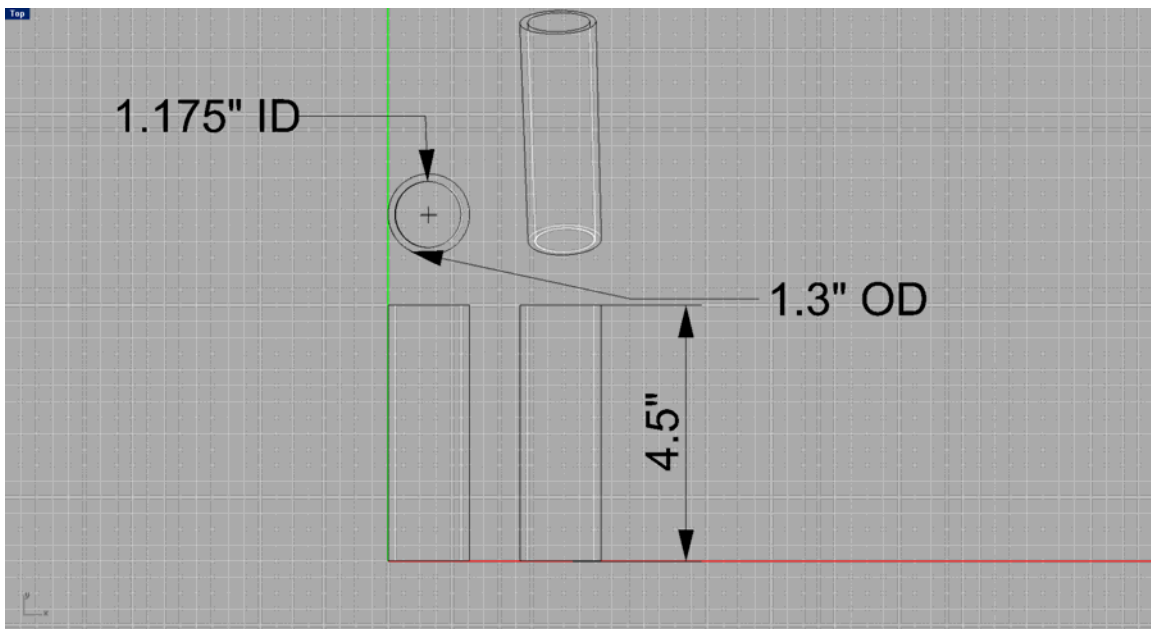


Figure 29. Tertiary electrode.

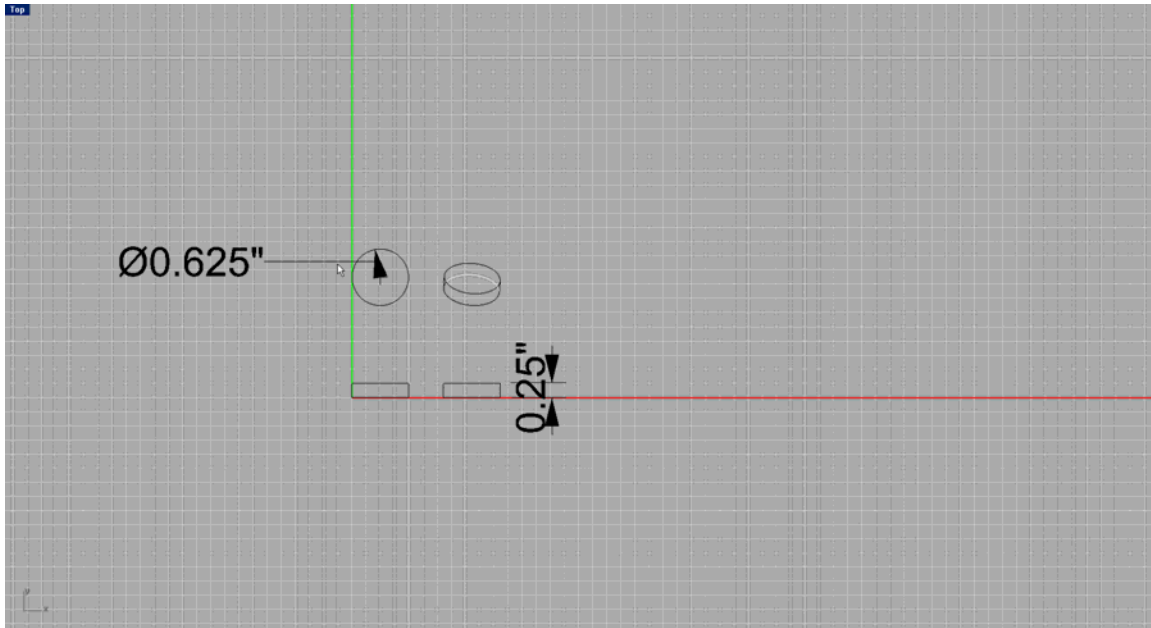


Figure 30. Top and bottom main electrodes.

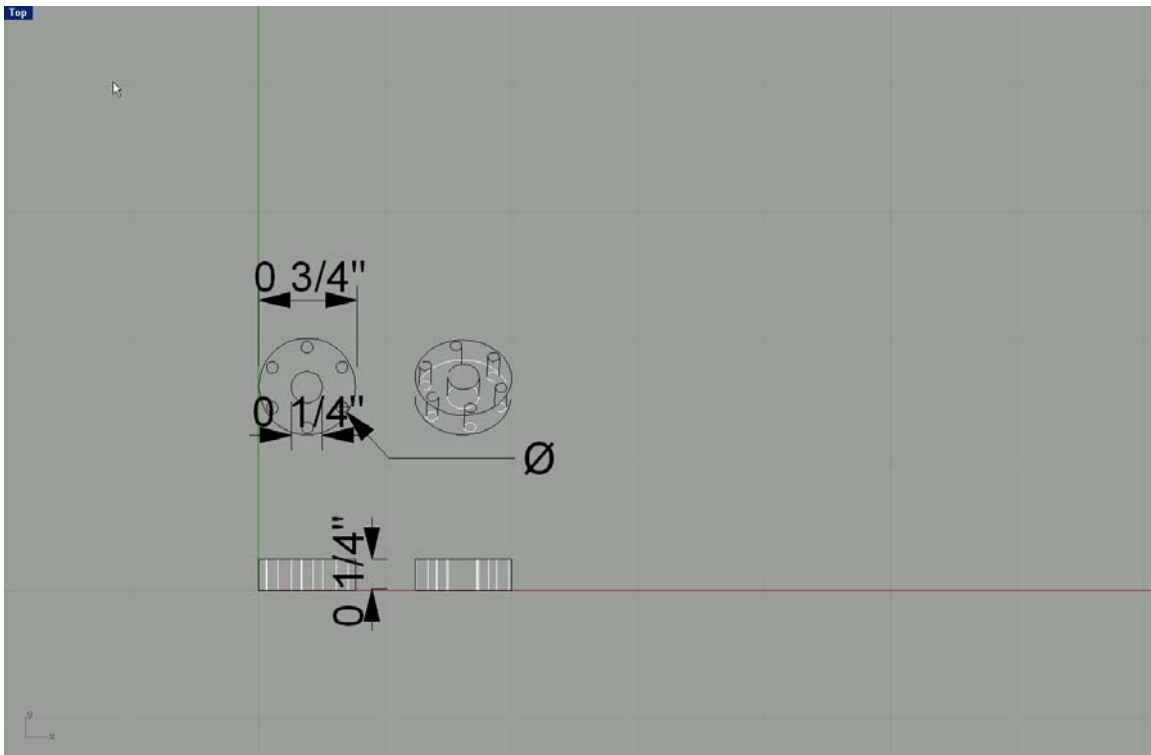


Figure 31. Top flange.

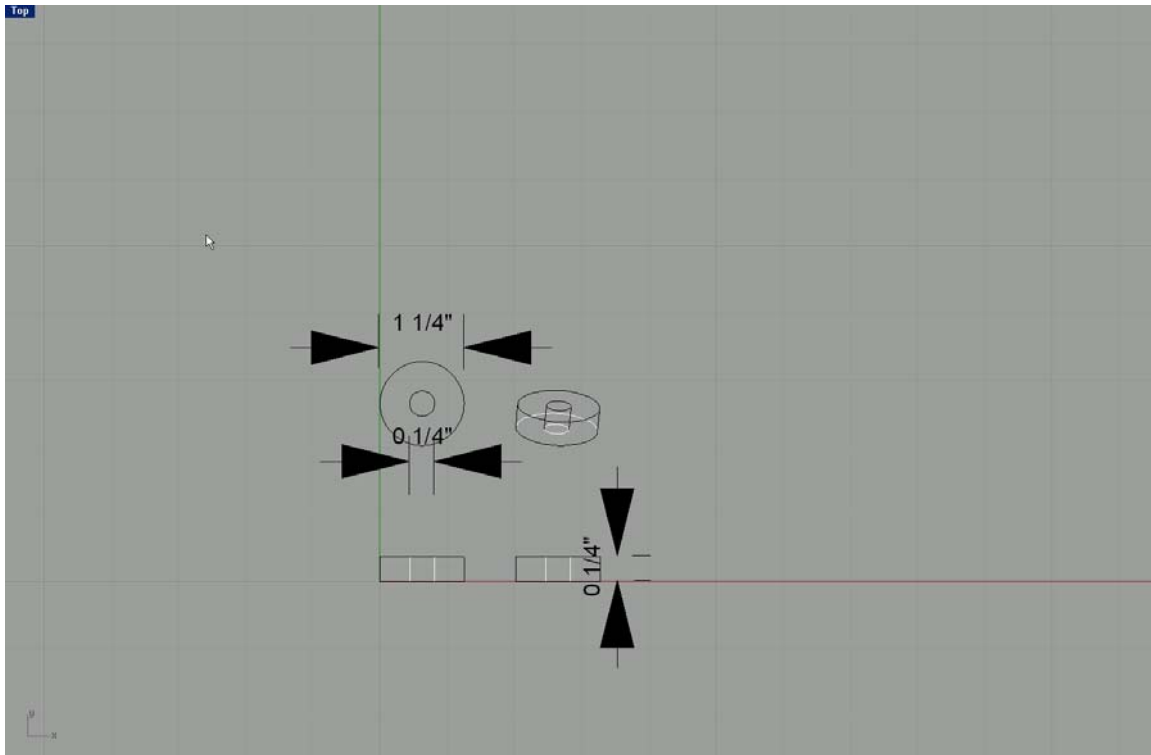


Figure 32. Second flange from top.

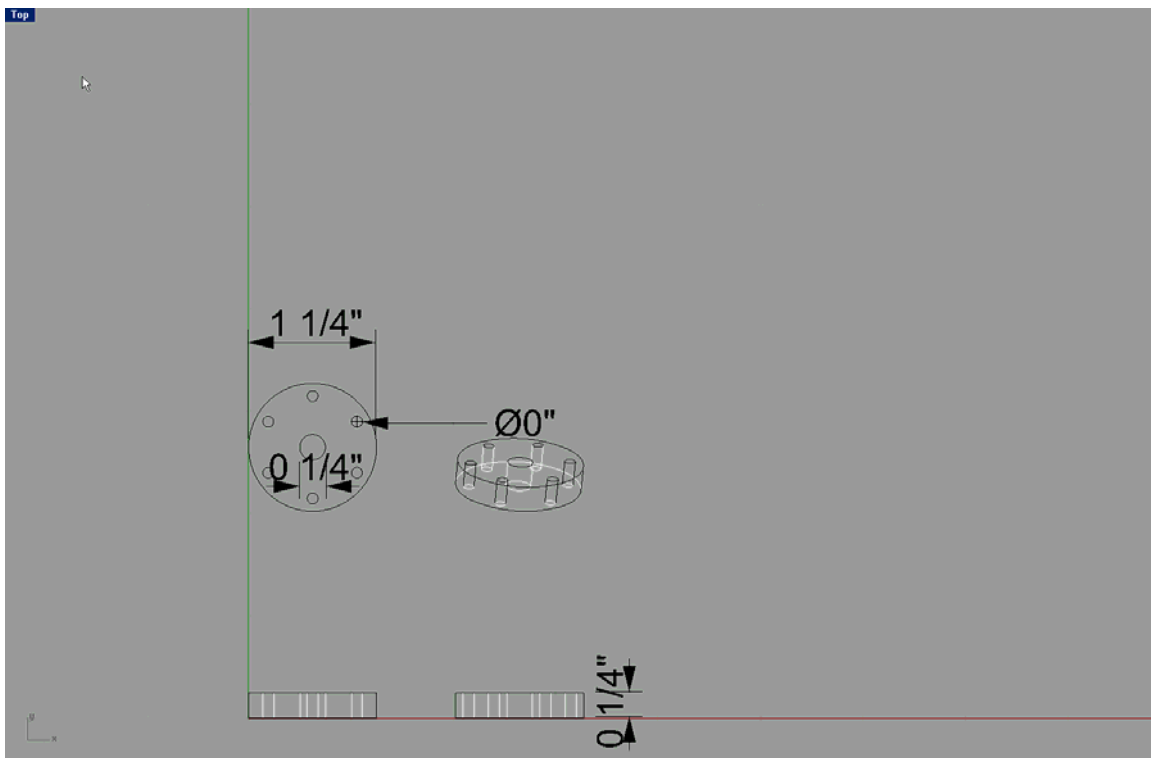


Figure 33. Third flange from top.

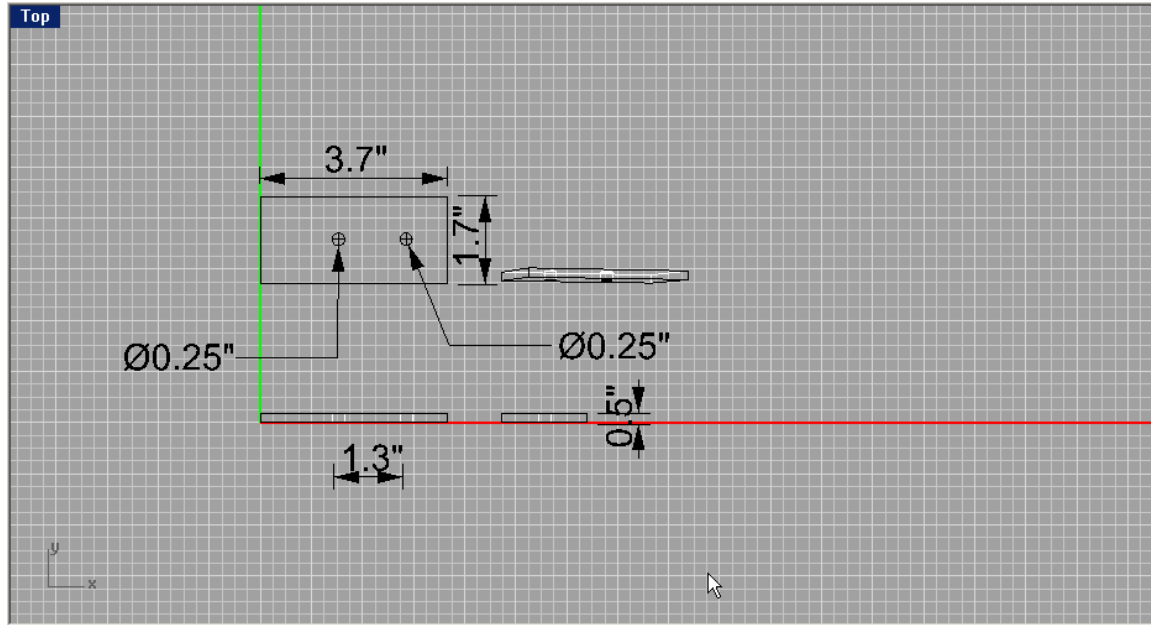


Figure 34. Mounting bottom plate w/ feed through hole and stationary rod hole.

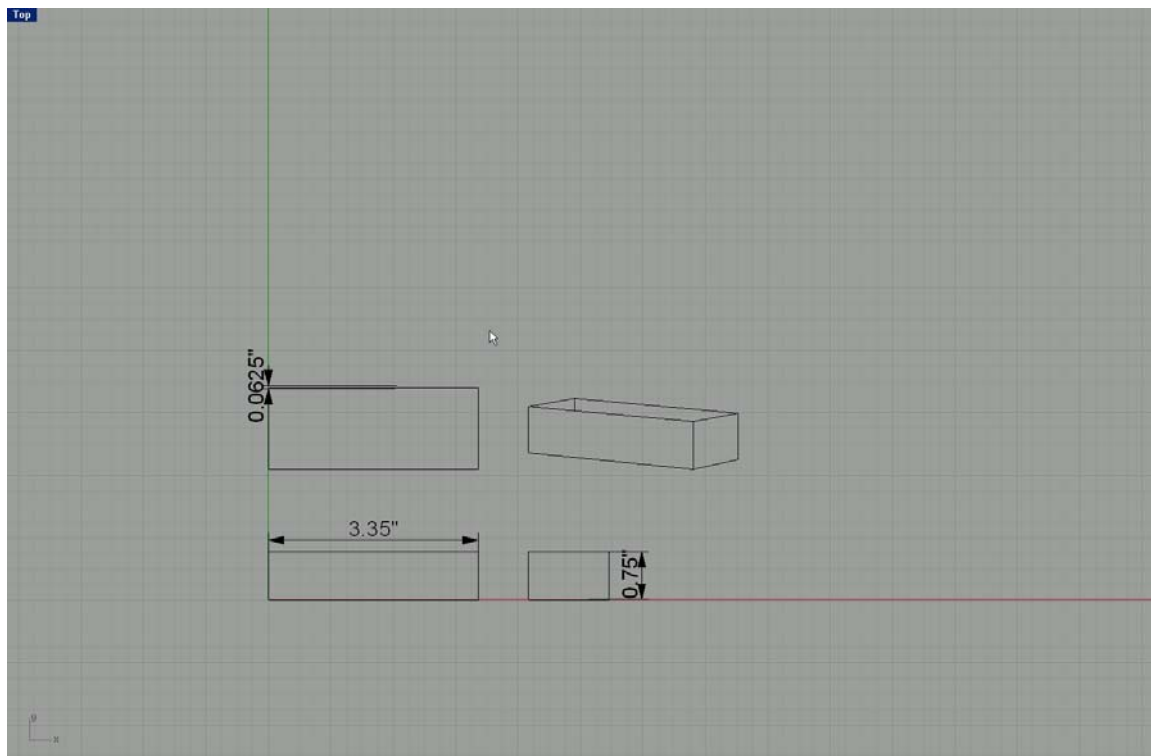


Figure 35. Bottom lower extension box.

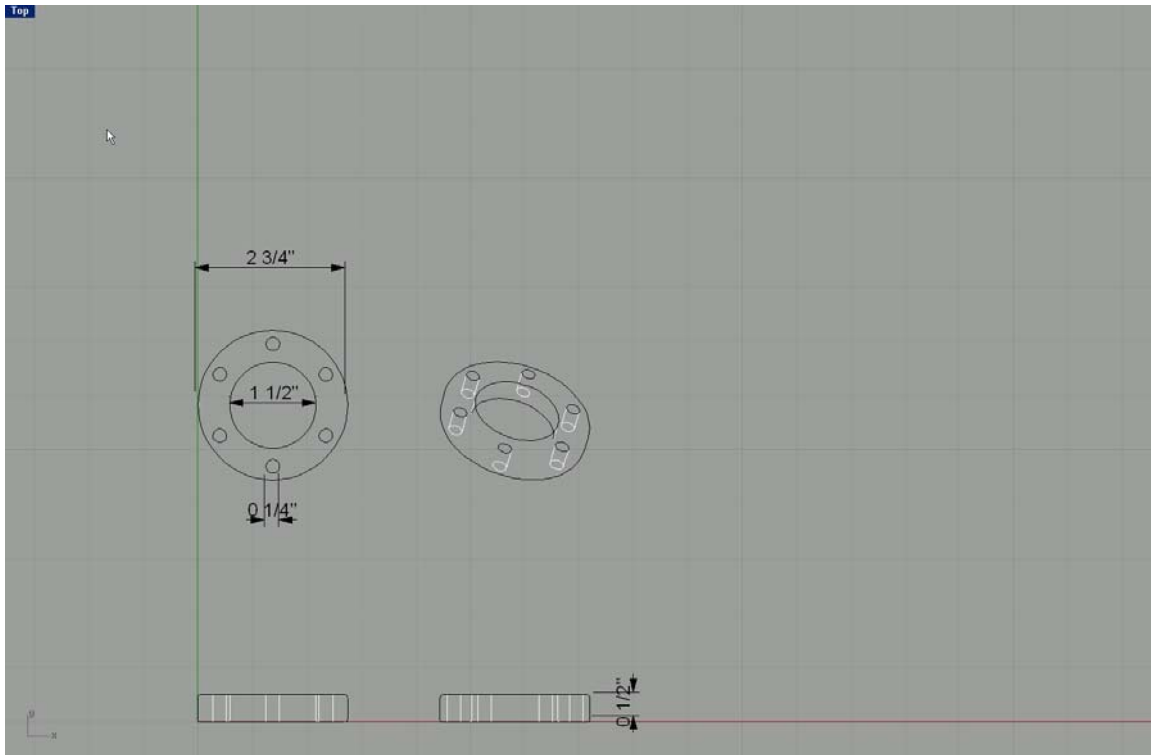


Figure 36. Bottom flange.

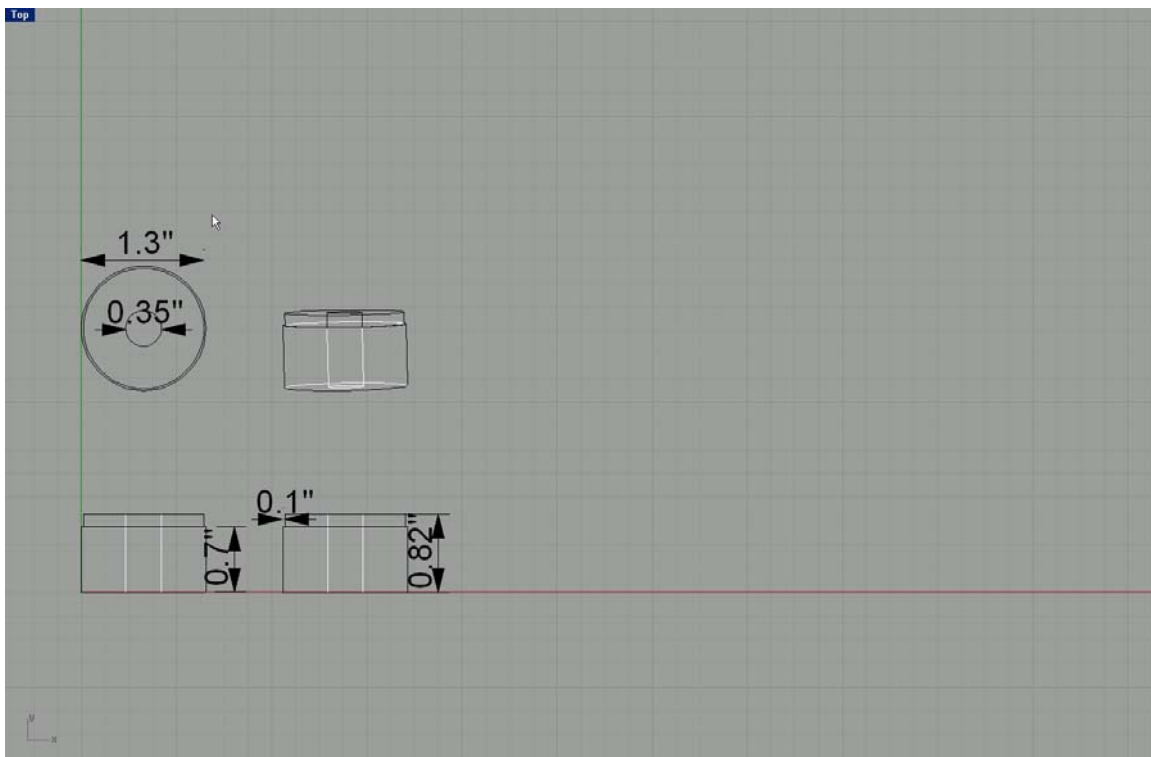


Figure 37. Top and bottom insulators.

THIS PAGE INTENTIONALLY LEFT BLANK

APPENDIX B. PROTOTYPE APPLICATION

PATENT DISCLOSURE

Double Pole High-Voltage High-Current Switch

Dagmara Moselle

831-649-0641

142 7th St, Pacific Grove, CA 93950

and

Don Snyder

PH/cw

831-656-2765

and

William Bryan Maier II

PH/mw

831-656-3227

305 Oak Circle, Marina, CA 93933

16 December 2005

Unclassified

A. DESCRIPTION OF THE PROBLEM(S) THE INVENTION ADDRESSES

The military's precision strike railgun will be able to provide direct and indirect fire support to the horizon or several hundred nautical miles within minutes. It will send high-muzzle-velocity projectiles to penetrate and destroy adversary targets. However, presently there remains no reliable and compact power source to provide the required power to drive the railgun for multiple consecutive shots. If there were an opening switch that would carry high currents ($>50\text{KA}$) for times greater than 0.1 seconds and could open against such high currents (circuit interruption), then better power supplies might be available for use in an operational railgun. This patent addresses a new switch design that can be used for the railgun power supply and for many other applications.

B. DESCRIPTION OF THE PRIOR ART TECHNOLOGY THAT DID NOT FULLY RESOLVE THE PROBLEM(S) ADDRESSED BY THE PRESENT INVENTION BUT THAT MAY HAVE COME CLOSE

Circuit interruption has been accomplished mechanically with solid state switches [2] and with hybrid switches [3], [4]. Only the hybrid switch is capable of circuit interruption at high currents and capable of conduction for greater than 0.1 seconds. For example, the commercially available vacuum interrupter can carry large currents for long periods but must open when the current is approximately zero or small [5].

There are mainly two ways to accomplish mechanical circuit interruption. One way is to suppress the rise in voltage across an opening switch after an arc gap is established, or secondly to increase the resistance of the plasma when the current is zero. Historically there have been several circuit breaker modes that impeded arcing in opening switch with the intent to extinguish current flow as quickly as possible. One of the first was an oil type. In this model, the oil molecules were generated as a result of the arcing and extinguished the plasma by deionization. (1) This design for the military is unsuitable because oil is a flammable hydrocarbon and would be a fire hazard. A second model used air to engulf the arc and quench the arc using the air's insulator qualities. (2) This switch type is acceptable in most situations, but has an inconsistent extinguishing time. Another circuit switch used an air blast process to put out the arc. (3) This switch design proved to be less desirable because switch operation depended heavily on nozzle placement and blast intensity and made the design parameters too specific. Lastly, a

modern successful circuit breaker uses vacuum to help condense the vapor between the electrodes to prevent re-striking. Vacuum circuit breakers are highly desirable because they have limited maintenance due to their clean vacuum environment and rather simple switch structure. They also require a small amount of energy to operate and are relatively silent so that they are a highly desirable switch. [1] Figure 1 depicts a commercial vacuum interrupter from ABB. None of these switches open well against high currents.

- 1 Stem/terminal
- 2 Metal bellows
- 3 Interrupter lid
- 4 Ceramic insulator
- 5 Shield
- 6 Contacts
- 7 Stem
- 8 Interrupter lid

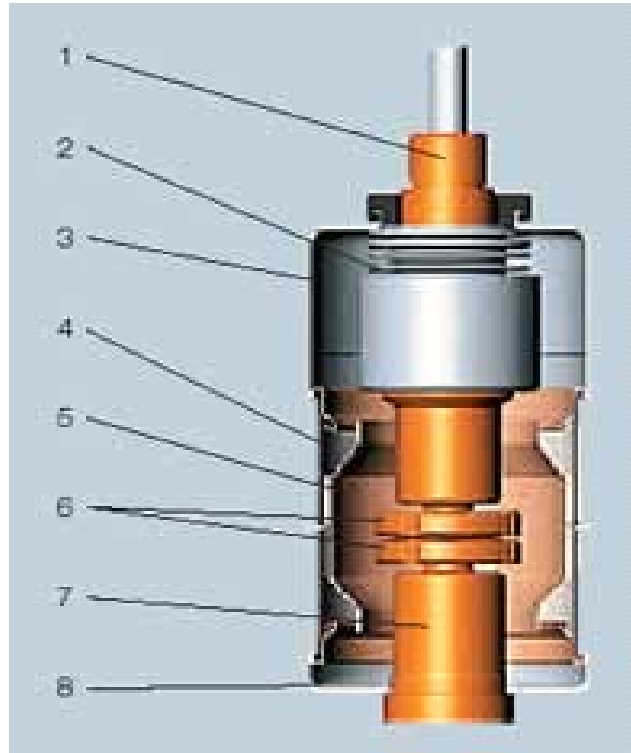


Figure 1- Basic Vacuum Interrupter taken from [5]

C. SCHEMATIC AND BRIEF STEP-BY-STEP DESCRIPTION AND EXPLANATION OF THE INVENTION

Due to the inherent electrical insulation of a vacuum, this double-pole switch described here is designed to operate under vacuum conditions. When the switch is closed, current will flow through the apparatus with minimal resistance providing power to the load as seen in Figure 2.

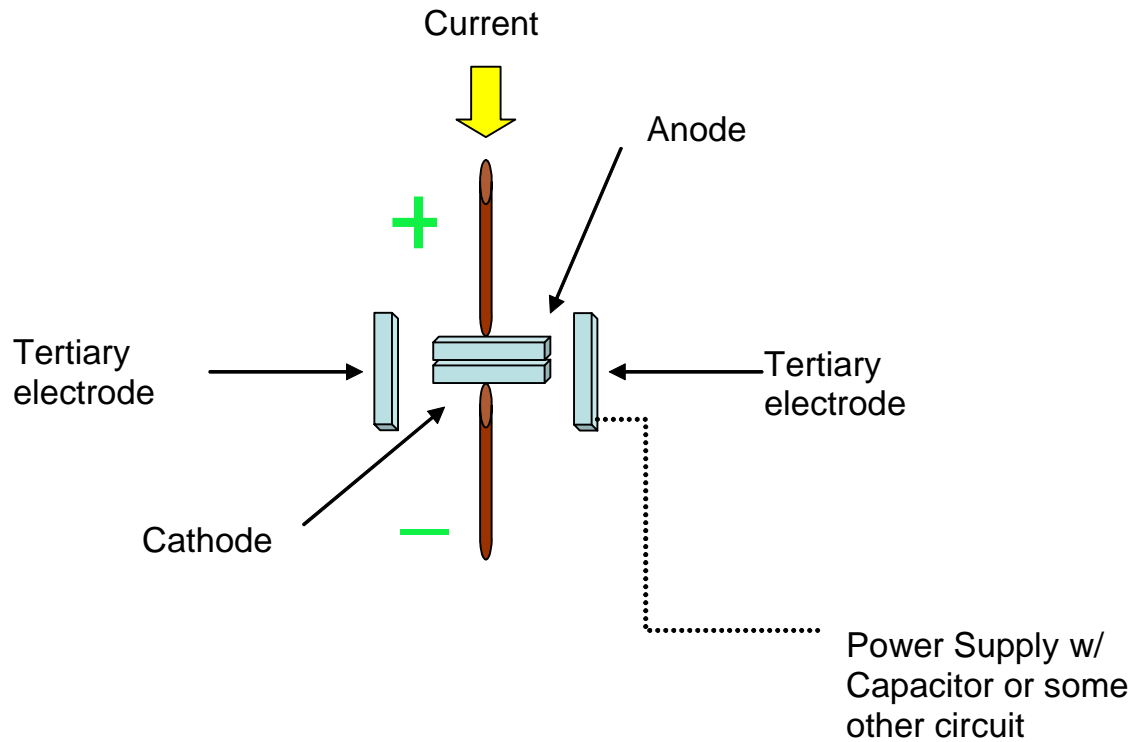


Figure 2-Closed Double Pole Switch

Subsequently, when the switch is opened, an arc (depicted in Figure 3) will start to develop between the main cathode and anode due to the rise in voltage caused by the sudden change in current in the circuit inductance.



Figure 3-Vacuum Arc between Two Electrodes [5]

In this double-pole switch, the electrons and ions in the plasma between the main cathode and anode will be diverted to a tertiary anode by an applied magnetic field, thus suppressing the arc and fully opening the switch. The magnetic field will cause the charged particles to spiral along the magnetic field lines. This change in direction of the electrons and charged particles occurs because the electric and magnetic fields are perpendicular. A simplistic schematic depicting the general principle of operation for this switch is given in Figure 4.

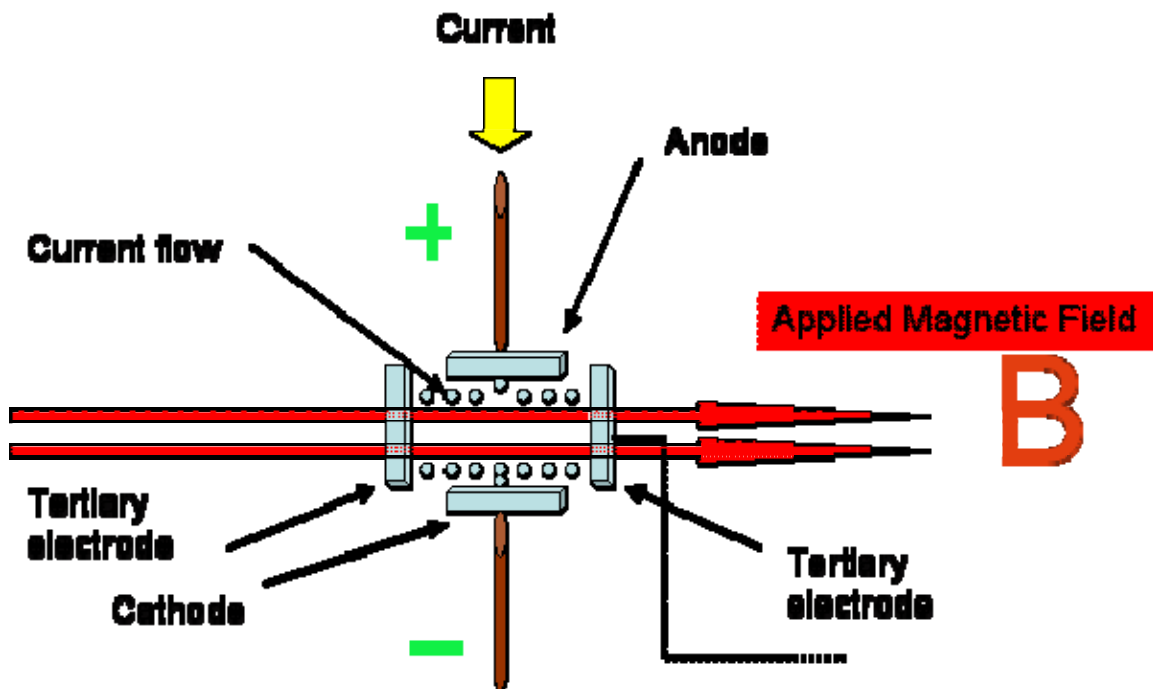


Figure 4-Opened Double-Pole Switch with Magnetic Field B Shown

The figure above is intended to show the concept of operation and not the exact configuration. If there had been no external magnetic field applied to direct the electrons and ion particles, the arc would remain developed and allow minimal current flow as demonstrated in Figure 5.

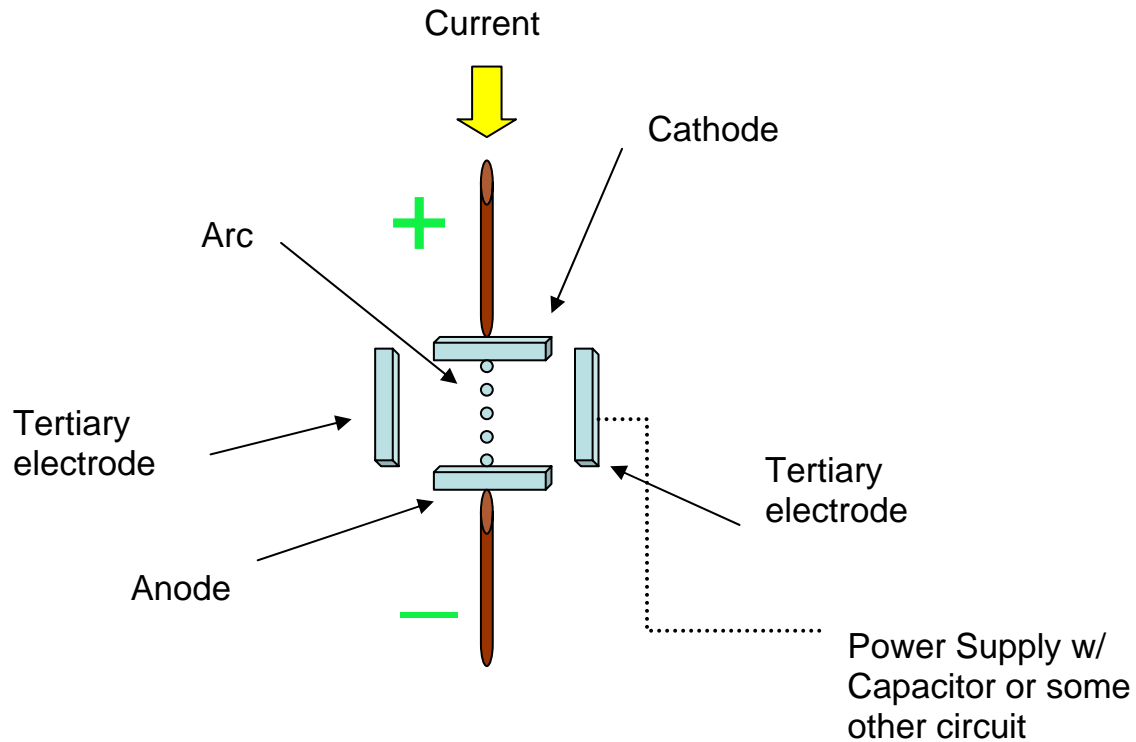


Figure 5-Current Flow in Opened Double-Pole Switch without Applied Magnetic Field

In one embodiment, the switch could appear like the design below in Figure 6 with an outer shield acting as the electron and/or ion absorber. There are many arrangements for this switch with the same concept, current diverted to a tertiary electrode by a magnetic field.

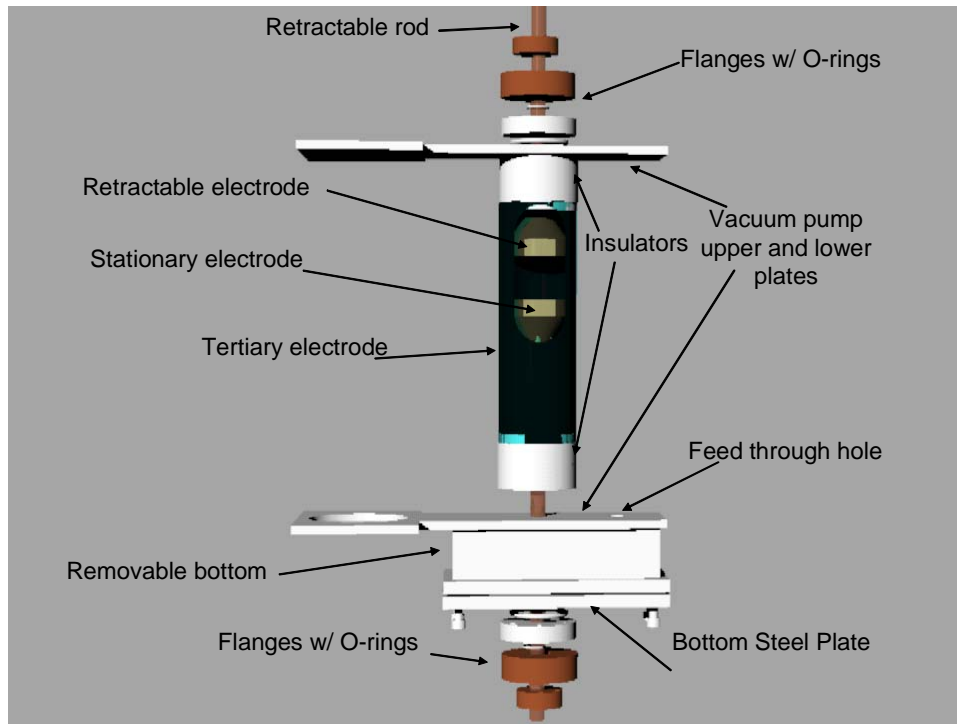


Figure 6

D. EXISTING PHOTOGRAPHS, DRAWINGS, SCHEMATICS, AND OTHER MATERIAL THAT PROVIDES INSIGHT TO THE INVENTION, HOW IT FUNCTIONS, AND WHAT IT DOES

No prior description of similar idea is known.

E. IN ANTICIPATION OF POSSIBLE COMMERCIAL LICENSING UNDER THE TECHNOLOGY TRANSFER ACT, PLEASE IDENTIFY ANY SPONSORS (GOV'T OR COMMERCIAL COMPANIES) KNOWN TO HAVE AN INTEREST IN THE INVENTION. PROVIDE ADDRESS AND GEOGRAPHICAL LOCATION IF KNOWN

This invention will be of interest to the US Army, US Navy and US Marines.

F. WAS THIS INVENTION DONE UNDER A COOPERATIVE RESEARCH AND DEVELOPMENT AGREEMENT?

No.

G. OTHER POTENTIAL USES BESIDES RAILGUN POWER SYSTEMS

Power systems where low voltage energy storage is converted to inductive storage to provide high voltage energy to drive a load.

H. NOTE ON OTHER EXISTING TECHNOLOGY

As the invention described was made as a direct result of the performance of my assigned duties, I agree to assign the entire right, title, and interest in the invention to the government and I understand that I will retain no rights in this invention.

LIST OF REFERENCES FOR PATENT

- [1] Flurschein, C.H. "Power Circuit Breaker Theory and Design," Institution of Electrical Engineers, 1975.
- [2] Pokryvailo, Yankelevich, and Shapira. "A Compact Source of Subgigawatt Subnanosecond Pulses," *IEEE Transactions on Plasma Science*, Vol. 32, No. 5, October 2004, pp. 1909-1917.
- [3] Pokryvailo, Ziv, and Shapira. "Repetitive Inductive Storage Supply for an ETC Tank Gun," *IEEE Transactions on Magnetics*, Vol. 39, No. 1, January 2003, pp. 257-261.
- [4] Pokryvailo, Ziv, and Shvro. "Status of 5 MW Inductive Storage Facility at Soreq NRC, *IEEE Digest of Technical Papers, Pulsed Power Conference* 2003, pp. 445-448.
- [5] ABB. Available at <http://www.abb.com>. As of 03NOV05.

APPENDIX C. LONG THIN SOLENOID

For a Long Thin Solenoid:

$$L = \frac{\mu_o N^2 A}{\ell} = \frac{\mu_o N^2 \pi r^2}{\ell} = \frac{\pi(4\pi \times 10^{-7} H / m)(9^2)(0.3m)^2}{0.5m} = 57.6\mu H$$

However, this is only an approximation because the inductor of interest is not long and thin. In fact, the inductor's length approaches the inductor's diameter.

THIS PAGE INTENTIONALLY LEFT BLANK

LIST OF REFERENCES

- [1] Telephone conversation between W. Maier and M. Crawford, The University of Texas at Austin Institute for Advanced Technology, Austin, TX, approximately 01 FEB 2003.
- [2] Maier, William B. *PH3994 Course Notes*, Naval Postgraduate School, Monterey, CA, 2005.
- [3] ABB. Available at <http://www.abb.com>. As of 03NOV05.
- [4] Pokryvailo, Ziv, and Shapira. "Repetitive Inductive Storage Supply for an ETC Tank Gun," *IEEE Transactions on Magnetics*, Vol. 39, No. 1, January 2003, pp. 257-261.
- [5] Pokryvailo, Kanter, Shaked. "A Two-Stage Opening Switch for Inductive Energy Storage Systems," *IEEE Transactions on Magnetics*, Vol. 34, No. 3, 1998, pp. 655-663.
- [6] Duniway Stockroom Corporation. Available at <http://www.duniway.com>. As of 01SEP05.
- [7] Flurscheim, C.H. "Power Circuit Breaker Theory and Design," Institution of Electrical Engineers, 1975.
- [8] Pokryvailo, Yankelevich, and Shapira. "A Compact Source of Subgigawatt Subnanosecond Pulses," *IEEE Transactions on Plasma Science*, Vol. 32, No. 5, October 2004, pp. 1909-1917.
- [8] Pokryvailo, Ziv, and Shvro. "Status of 5 MW Inductive Storage Facility at Soreq NRC, *IEEE Digest of Technical Papers, Pulsed Power Conference* 2003, pp. 445-448.

THIS PAGE INTENTIONALLY LEFT BLANK

INITIAL DISTRIBUTION LIST

1. Defense Technical Information Center
Ft. Belvoir, Virginia
2. Dudley Knox Library
Naval Postgraduate School
Monterey, California
3. William B. Maier II
Physics Department
Code PHMW
Naval Postgraduate School
Monterey, California
4. CAPT David Kiel
PMS 405
Naval Sea Systems Command
Washington Navy Yard
Washington, DC
5. CAPT Roger McGinnis
Director, Air Warfare and Naval Weapons Applications Division
ONR 352
Office of Naval Research
Arlington, Virginia
6. Gene Nolting
PMS 405
Naval Sea Systems Command
Washington Navy Yard
Washington, DC
7. Chester Petry
Naval Surface Warfare Center, Dahlgren Division
Naval Sea Systems Command
Dahlgren, Virginia
8. Ian McNab
Institute for Advanced Technology
The University of Texas at Austin
Austin, Texas

9. Prof. Hans Mark
WRW 401C
Institute for Advanced Technology
The University of Texas at Austin
Austin, Texas